

5. RESULTS AND DISCUSSION

This chapter describes the results of study carried out to meet the objectives mentioned earlier. These results have been discussed in the light of relevant literature.

5.1 Identification of the diversity of the biofouling lower plants and cyanobacteria with their specific substratum

A total of 36 species of biofoulants have been isolated and identified from the samples of different groups collected during the study. These include 10 species of cyanobacteria, 1 species of microalgae, 17 bryophyte species and 8 species of lichens from the selected monument sites.

5.1.1 Cyanobacteria and Microalgae

Eleven species of microorganism were recorded on the biofilms that were isolated from the monuments. Among them, 6 cyanobacteria species constituted the dominant biofilm component on the monument sites investigated while the other five species were found in association with them.

5.1.1.1 Culturing and optimization

Isolation of the dominant six species was done through streak plate method and individual colonies were picked up from the agar plates to obtain their monoculture in broth. Fig. 5.1 depicts the streaked plates of mixed and pure cultures of biofilm samples while fig. 5.2 represents the pure cultures in broth obtained from individual colonies picked up from the agar media. In fig. 5.2, images A to F show the culture of different species (*Nostoc punctiforme*, *Leptolyngbya foveolarum*, *Asterarcys quadricellulare*, *Desmonostoc muscorum*, *Leptolyngbya crispata*, *Chroococidiopsis cubana*). A large biomass of these pure cultures were required for molecular and other studies and this proved to be a challenging task. There was a need of optimization of the main components of the media for increased yield. Optimization studies were thus done on one species. A single colony of *Chroococidiopsis cubana* grown in control and experimental flasks for 10 days. Table 5.1 and fig. 5.3 depicts the flasks of the different experimental setups undertaken. Their range and levels of variables have been given earlier in methodology section under table 4.6. Flask indicated at setup 1 was the control and the remaining flasks 2 to 13 were different experimental setups. Table 5.1 also depicts the yield recorded. Except setup 4, the biofilm yield of all experimental flasks were significantly higher than of control.

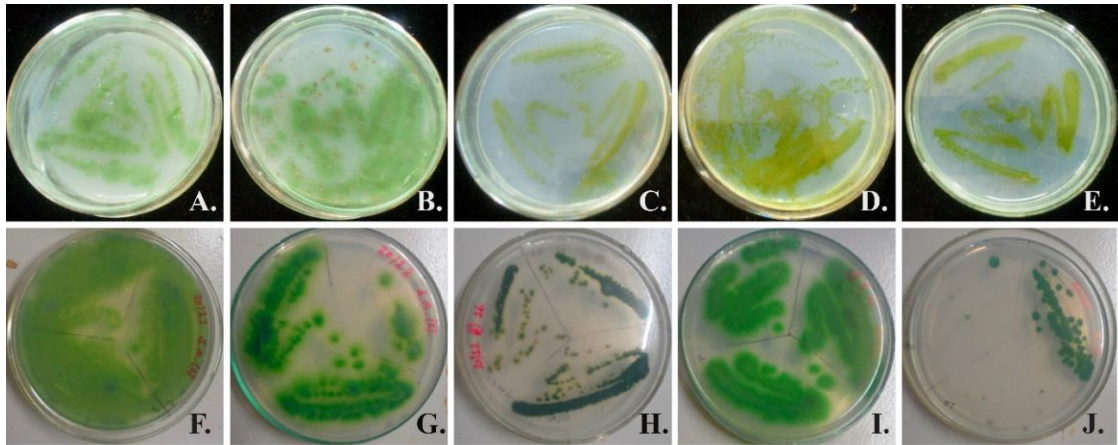


Fig. 5.1 – Cyanobacterial biofouling isolates by streak plate method

A. to E. Mix culture colonies and F. to J. Pure culture colonies

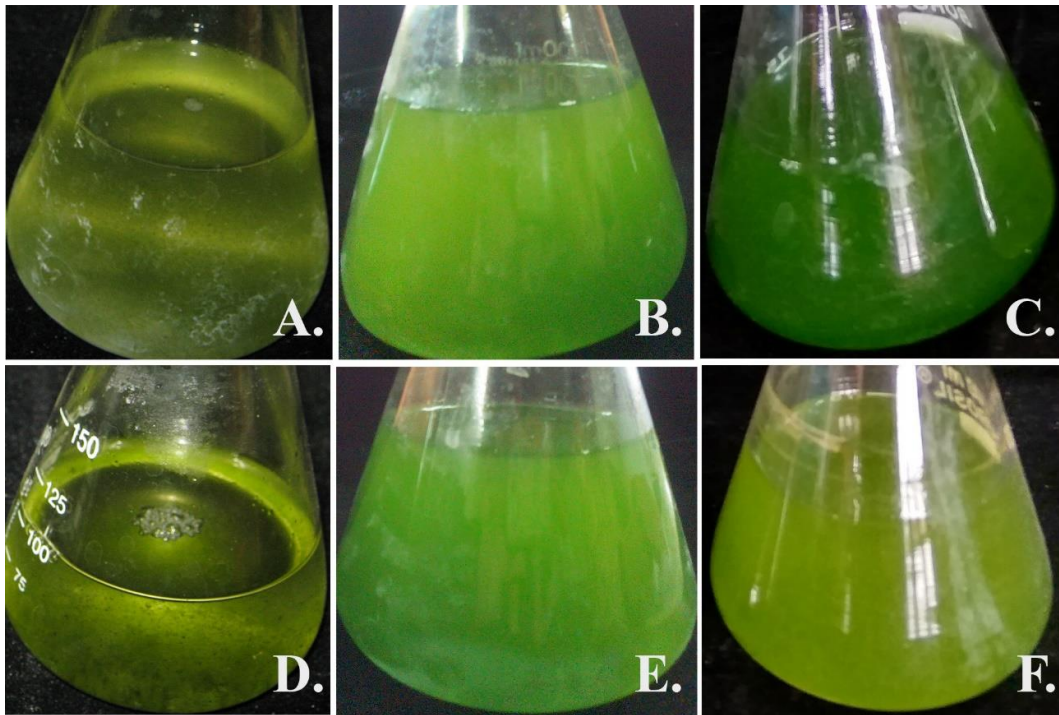


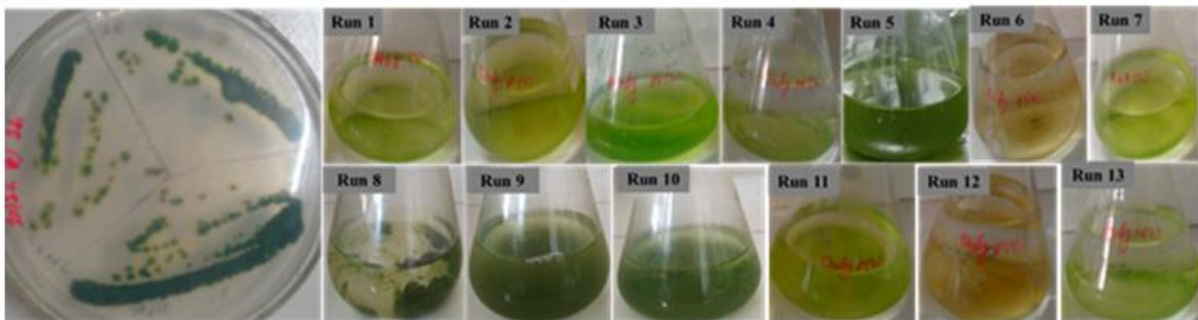
Fig. 5.2 – Cyanobacterial biofouling monoculture in broth

A. *Nostoc punctiforme*, **B.** *Leptolyngbya foveolarum*, **C.** *Asterarcys quadricellulare*, **D.** *Desmonostoc muscorum*, **E.** *Leptolyngbya crispata*, **F.** *Chroococcidiopsis cubana*

Biodeterioration of Selected Historical Monuments by Lower Plants and Cyanobacteria

Table 5.1 – Experimental design with experimental yield (at 10th day)

Experimental Set up	X ₁ (B)	X ₂ (A)	Biofilm yield(g/l)
1	-2	0	10
2	2	0	18
3	0	0	20
4	-1	1	05
5	0	0	20
6	0	2	10
7	-1	-1	16
8	0	0	20
9	0	0	20
10	0	0	20
11	1	1	19
12	1	-1	12
13	2	-2	15



A. Isolation by streak plate method

B. Experimental setup design by Central Composite design

Fig. 5.3 – Isolation and experimental set up of CCD in lab for optimization

5.1.1.2 ANOVA for Response surface model

The effect of two independent variables variable A (NaNO₃) and variable B (K₂HPO₄) were studied on one dependent response (Yield of the Culture). The results of the second order response surface model for increase yield based on analysis of variance (ANOVA) is given in Table 5.2. Regression equation of yield having empirical function of test variables in coded unit is shown in equation 5.1:

$$\hat{Y}_i = 20 + 2.66X_1 - 1.38X_2 + 4.50 X_1X_2 - 3.06 X_1^2 - 3.81 X_2^2 \dots\dots\dots \text{Equation 5.1}$$

Where \hat{Y}_i is the predicted yield, X₁ is K₂HPO₄ and X₂ is NaNO₃

ANOVA uses F – statistic to test the equality of means. F – test had very low probability value [(Prob>F) < 0.0001]. Hence, this model was highly significant for this experiment. Goodness of fit of model was determined by determination coefficient (R²). The R² value was 0.99 owing to which 99 % sample variation was qualified the variables, only 1% of the total variance could not be explained by this model. Adjusted determination coefficient also had similar value. Hence, the significance of the model was confirmed at the required confidence level of 99%. The standard deviation (SD) was 0.47. A small value of the SD would generally mean more precise data while a larger value of SD would also increase the acceptable range within the data variability. Coefficient of variation or pure error was 2.95%. As this was lower than 5% it fell within the acceptable range. The adequate precision, which measures the signal to noise ratio and for which a value greater than 4 is desirable. This value obtained for the current model was 48.72. Because the model had a high signal, it was considered more reliable for optimization. Table 5.2 below depict the parameters and results obtained.

Table 5.2 – ANOVA for response surface quadratic model

Source	Sum of Square	Degree of freedom	Mean Square	F – value	Probe>F (p value)
Model	300.79	5	60.16	277.10	<0.0001
Residual	1.52	7	0.22		
Lack of fit	1.52	3	0.51		
Pure error	0.00	4	0.00		
Total	302.31	12			

Standard deviation. = 0.47; Coefficient of variation = 2.95%; Mean = 15.77; R² = 0.99; Adj. R² = 0.99; Pred. R² = 0.96

5.1.1.3 Coefficient estimation for model

The significance of coefficient was determined by t value and p value. Both these values were computed and have been mentioned in Table 5.3. The results are considered to be more significant when the value of t-test is higher and the p value is smaller. Our model intercept had a large t value suggesting that this model was highly significant. In the model, variable A had a smaller p value as compare to variable B. Hence variable A was more significant than variable B in this model. The 2D contour plot represents graphical view of the regression equation. It had shown the effect of both the variables on yield of biofilm. Based on centre point of the contour plot, the obtained value of variable A (NaNO₃) and variable B (K₂HPO₄) were 13 and 6.5 respectively (Fig 5.4). Hence, both these values were found to be optimal for biofilm yield in 10 days. For optimization, the Design Expert 7.0.2 software suggested 0.95 and 1 as the two desirability standards. In current study, we proceeded for desirability 1 and the obtained value for A (NaNO₃) = 13 (with the lower and upper limits as 10 and 15 respectively) and value for B (K₂HPO₄) = 6.5 from (with the lower and upper limits as 5 and 8 respectively). This gave a yield of 20 g/l yield in 10 days.

Table 5.3 – Coefficient estimation of model

Factor	Coefficient	Std. error	Computed t – value	Computed p - value
Intercept	20	0.21	95.23	0.003
A	2.66	0.16	16.625	0.019
B	-1.38	0.16	-8.625	0.036
AB	4.50	0.23	19.57	0.016
A ²	-3.06	0.18	-17.0	0.018
B ²	-3.81	0.18	-21.0	0.015

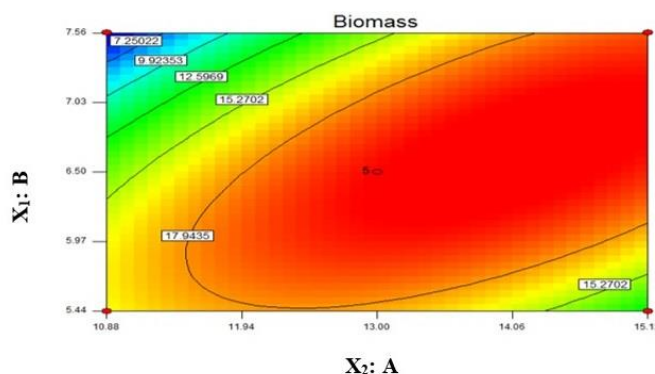


Fig. 5.4 – 2D contour plot for *in vitro* biofilm yield of *Chroococcidiopsis cubana*

5.1.1.4 Molecular study by 16S rRNA marker

The identity of the cultures of the isolated strains were confirmed by 16S rRNA gene sequences. The DNA band image of the different strains is shown in fig. 5.5. Sanger sequencing data were obtained using purified amplicon of each strains of biofoulants. The BLAST analysis of sequence data helped reveal the identity of the isolated strain. In addition to the microscopic morphological features, the 16S rRNA gene sequence data were considered during the confirmation of the strain. The six species belonging to five different genera were identified as *Leptolyngbya foveolarum* and *Leptolyngbya crispata* (both members of Synechococcales), *Desmonostoc muscorum* and *Nostoc punctiforme* (both members of Nostocales), *Chroococcidiopsis cubana* (Chroococcidiopsidales), *Asterarcys quadricellulare* (Chlorococcales) (Mehta and Shah, 2021). All strains sequences data were deposited in NCBI GenBank data base and their accession numbers were obtained (Table. 5.4).

Table 5.4 – Biofoulants with their GenBank Accession No.

Sr. No.	Name of the organisms	GenBank Accession No.
1.	<i>Chroococcidiopsis cubana</i>	MN950976
2.	<i>Desmonostoc muscorum</i>	MN950971
3.	<i>Nostoc punctiforme</i>	MN950972
4.	<i>Leptolyngbya foveolarum</i>	MN950974
5.	<i>Leptolyngbya crispata</i>	MN969628
6.	<i>Asterarcys quadricellulare</i>	MN955451

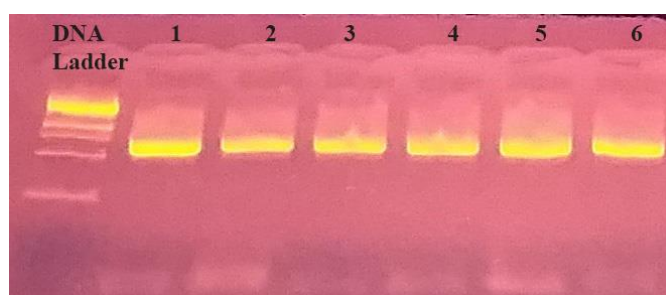


Fig. 5.5 – DNA band images of each strains (1 - 6) by 16S rRNA marker

Remaining associated species from biofilm were observed and identified using morpho-taxonomy. From that five associated cyanobacterial biofoulants belonging to four genera from the order Chroococcales (*Gloeocapsa*, *Gloeocapsopsis*, *Chroococcus* and

Biodeterioration of Selected Historical Monuments by Lower Plants and Cyanobacteria

Aphanothece). All over, six biofoulants were found from the selected monuments of Champaner-Pavagadh and eight from the selected monument of MSU. The biofoulants of monuments of Champaner-Pavagadh included two species (single genus) from the order Synechococcales (*Leptolyngbya*) as well as Nostocales (*Nostoc*) and single species from the order Chroococciopsidales (*Chroococciopsis*), and Chlorococcales (*Asterarcys*). The cyanobacterial biofoulants from monuments of MSU included five species belonging to four genera from the order Chroococcales (*Gloeocapsa*, *Gloeocapsopsis*, *Chroococcus* and *Aphanothece*) and one species each from the orders Chroococciopsidales (*Chroococciopsis*), Nostocales (*Nostoc*) and Synechococcales (*Leptolyngbya*). All these identified species have been given in table 5.6. The present study revealed that the members of Chroococcales were dominant on building of MSU campus while the members of Synechococcales and Nostocales dominated the monuments of Champaner-Pavagadh.

Table 5.5 – Diversity and distribution of cyanobacteria and micro green algae on selected monuments

Sr. No.	Name of the biofoulants	Selected monument sites							
		Champaner Pavagadh						MSU campus	
		1	2	3	4	5	6	7	8
Cyanobacteria									
1.	<i>Chroococciopsis cubana</i> Komarek & Hindak	+	+					+	
2.	<i>Leptolyngbya foveolarum</i> (Montagne ex Gomont) Anagnostidis et Komarek				+	+		+	
3.	<i>Leptolyngbya crispata</i> (Playfair) Anagnostidis & Komarek			+					
4.	<i>Nostoc punctiforme</i> (Kutz.) Hariot				+	+			
5.	<i>Desmonostoc muscorum</i> Agardh ex Bornet & Flahault			+				+	
6.	<i>Chroococcus varius</i> A. Braun								+
7.	<i>Chroococcus prescottii</i> Drouet and Daily								+
8.	<i>Gloeocapsa palea</i> (Kutzing)								+
9.	<i>Gloeocapsopsis crepidinum</i> (Thuret) Geitler ex Komarek								+
10.	<i>Aphanothece stagnina</i> (Sprengel) A. Brown								+
Microalgae									
1.	<i>Asterarcys quadricellulare</i> (K. Behre) E. Heggewald & A.W.F. Schmidt							+	

1. Saher ki Masjid, 2. Mandavi, 3. Amir Manzil, 4. Makai Kothar, 5. Navlakha Kothar, 6. Jain Temple, 7. Arts Dome, 8. D. N. Hall

5.1.1.5 Account wise cyanobacteria and microalgae species

The important differentiating characters observed under microscope have been mentioned below. Based on these main taxonomic features, species identification was facilitated. Moreover, supportive specific references with their figures were cited before the individual species description.

***Chroococidiopsis cubana* Komarek & Hindak (Pl.4 – Fig. E)**

(Keshari & Adhikary, 2013; p.530; fig.4)

Cells in small group, blue green colour, spherical to hemispherical, colourless sheaths, 3.5 μm length and 3.5-3.7 μm width.

***Leptolyngbya foveolarum* (Montagne ex Gomont) Anagnostidis et Komarek (Pl.4 – Fig. C)**

(Barberousse H. *et al.*, 2006; p.96, fig. 37 & 74)

Filament straight; Cells 3 μm in length and 1.5 -2 μm in width, sheath unlamellated; trichomes constricted at the cell wall; round end.

***Leptolyngbya crispata* (Playfair) Anagnostidis & Komárek (Pl. 4 – Fig. D)**

(Flechtner *et al.*, 2008; p. 422, fig 29)

Filaments with single and double false branching, with only 1 trichome per sheath, 4-6 μm wide. Sheath soft, colourless. Trichomes not tapering, slightly constricted at the cross-walls. Cells with thylakoids peripheral along the out- side walls and cross-walls, 1-2 μm long. End cells hemispherical, bluntly rounded, up to 3 μm long.

***Nostoc punctiforme* (Kutz.) Hariot (Pl. 4 – Fig. B)**

(Flechtner *et al.*, 2008; p. 425, fig. 51)

Trichomes densely arranged in the colonies, 4-5 μm in diameter. Cells spherical 4-6 μm long. Heterocytes observed, but very sparse, 4-5 μm in diameter, 4-5 μm long.

***Nostoc muscorum* Agardh ex Bornet & Flahault (Pl.4 – Fig. A)**

(Desikachary, 1959; p. 385, pl. 70, fig.2)

Synonym: *Desmonostoc muscorum* Agardh ex Bornet & Flahault

Thallus gelatinous-membranous, olive green in colour; filaments densely entangled and long; sheath distinct only at the periphery of the thallus; trichome 3-5 μm broad; cells short barrel shaped to cylindrical, up to twice as long as broad; heterocyst nearly spherical, 6-7 μm broad.

***Chroococcus varius* A. Braun (Pl.5 – Fig. C)**

(Desikachary, 1959; p. 107, pl. 24, fig.5)

Single or 2-4 cells together, seldom more in small or big groups, irregularly arranged, globular, without sheath 2-4 μm , with sheath 4-8 μm diameter., pale blue or olive green; sheath apparently thick, indistinctly lamellated, colourless or yellowish or pale orange yellow.

***Chroococcus prescottii* Drouet and Daily (Pl.5 – Fig. D)**

(Das & Adhikary, 2014; p.45; pl.2; fig.3)

4 cells in rectangular shape, cells hemispherical with blue green colour, lamellated envelope, 6-7 μm in diameter.

***Gloeocapsa palea* (Kutzing) (Pl.5 – Fig. B)**

(Das & Adhikary, 2014; p.45; pl.2; fig.3)

Cells 4 spherical or hemispherical, envelope around the cells distinct with 1-2 layers, cells 7-8 μm long and 3-4 μm broad.

***Gloeocapsopsis crepidinum* (Thuret) Geitler ex Komarek (Pl.5 – Fig. A)**

(Adhikary *et al.*, 2015; p.71, pl. 2, fig. 4)

Thallus gelatinous and soft but it became blackish hard film when dried; 2-4 cells in groups, rarely more, colony spherical or oval, 12-24 μm diameter, cells 4-8 μm in diameter, cells in groups of 4 or more carcinoid aggregates, thin yellowish, brownish or colourless sheath, sheaths unlamellated.

***Aphanothece stagnina* (Sprengel) A. Brown** (Pl.5 – Fig. E)

(Desikachary, 1959; p. 137, pl. 21, fig.10)

Cells oblong, more or less ovoid or cylindrical, 3-6.5 μm broad, 4.5 -11 μm long, more or less blue green, densely or sparsely arranged, without individual envelopes, homogeneous mucilage.

***Asterarcys quadricellulare* (K. Behre) E. Hegewald & A.W.F. Schmidt** (Pl. 4 – Fig. F)

(Hong *et al.*, 2012; p.199, fig. 1)

Cells in three-dimensionally arranged coenobia. The coenobia consisted of randomly distributed (1, 2, 4 or more) cells within a spherical mucilage envelope. Diameter varied from 3-4 μm up to 20 μm depending on the growth stage. However, it was very difficult to accurately classify the isolate by comparing morphological characteristics shared with other algae.

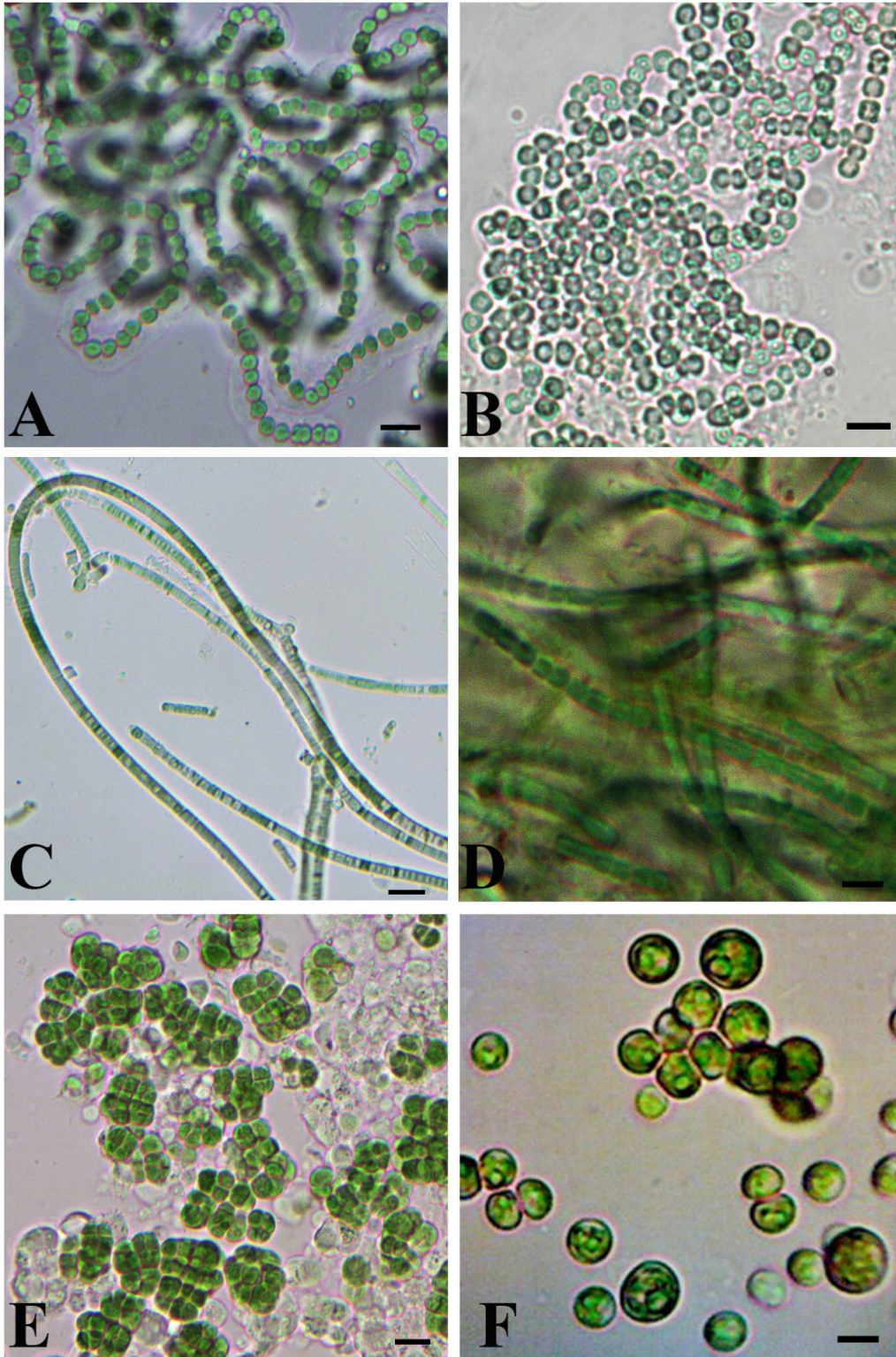


Plate 4 – Isolated organisms from the collected biofilm

A. *Desmonostoc muscorum*, B. *Nostoc punctiforme*, C. *Leptolyngbya foveolarum*, D. *Leptolyngbya crispata*, E. *Chroococcidiopsis cubana*, F. *Asterarcys quadricellulare* (Scale bars for all images = 10 µm)

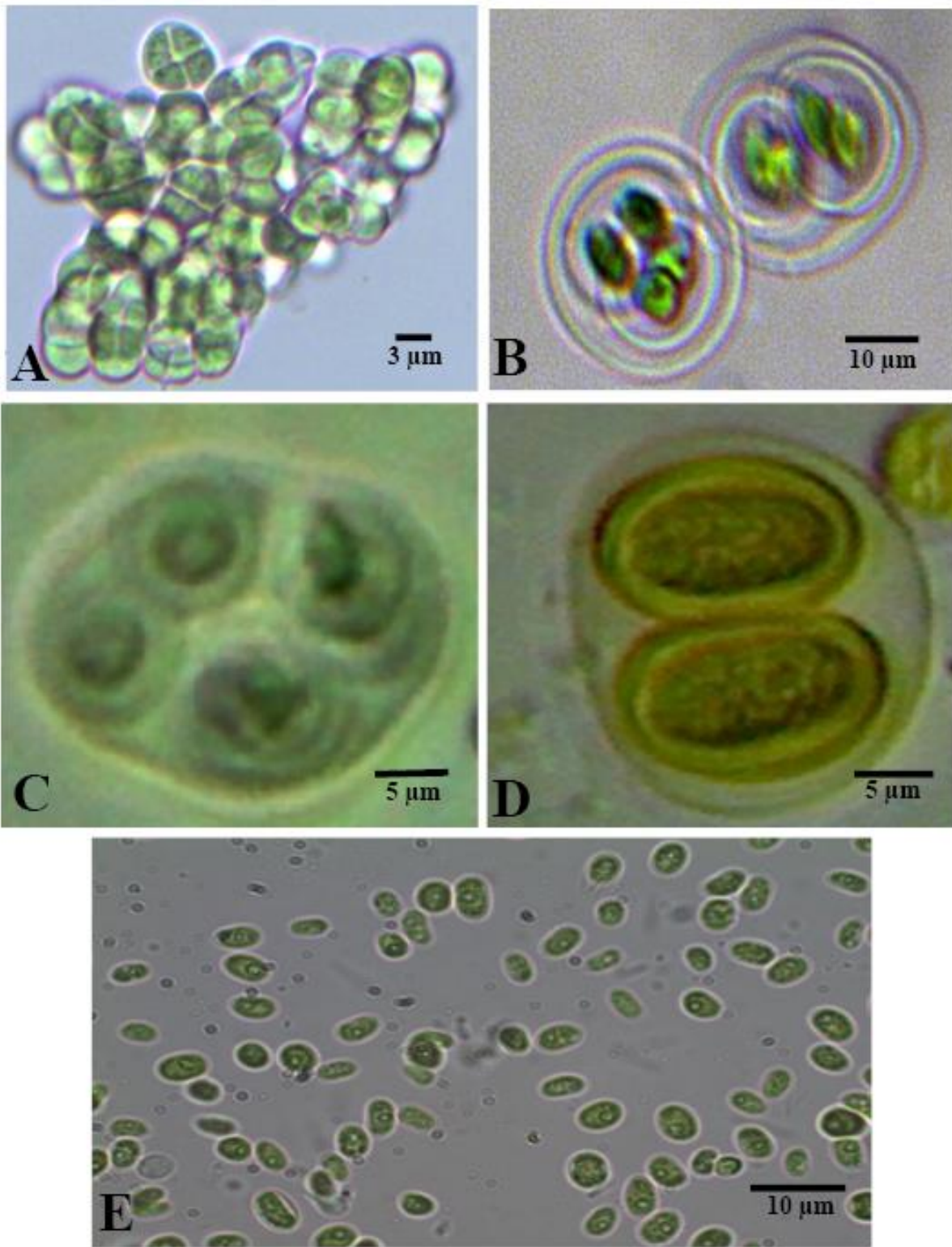


Plate 5 – Associated organisms with dominant organisms from collected biofilm

A. *Gloeocapsopsis crepidinum*, B. *Gloeocapsa palea*, C. *Chroococcus varius*, D. *Chroococcus prescottii*, E. *Aphanothece stagnina*

5.1.1.6 Status of cyanobacteria and green microalgae on monuments

In the current study, members of Synechococcales (*Leptolyngbya*) and Nostocales (*Nostoc*) were dominant on the biofilms of the selected monuments of Champaner Pavagadh. While members of Chroococcales (*Gloeocapsa*, *Gloeocapsopsis*, *Chroococcus* and *Aphanothece*) were dominant on the biofilm of the selected monuments of MSU campus. Studies on different monuments spread across various parts of India have also documented comparable results. These include studies by Samad and Adhikary (2008) on the monuments of Orissa recorded dominant species from the order Chroococcales genera namely *Chroococcidiopsis*, *Gloeocapsa*, *Gloeothece*, *Chroococcus*, *Aphanothece*, *Asterocapsa*, *Cyanosarcina*, *Gloeocapsopsis*, *Cyanothece*. Study by Keshari and Adhikary (2013) on the monuments of Shantiniketan (West Bengal) recorded mainly species of the orders Nostocales and Chroococcales. Three species of the genus *Nostoc* and one species of each genera *Gloeocapsa*, *Aphanothece*, *Gloeothece*, *Aphanocapsa*, *Chroococcus* and *Chroococcidiopsis* from the order Nostocales and Chroococcales respectively were documented. While *Lyngbya* species of the order Synechococcales were dominant on the monuments of Tamilnadu (Bhavani *et al.*, 2013).

Globally, genera namely *Chroococcus*, *Gloeocapsa*, *Gloeothece* from the orders Chroococcales; two species of genus *Leptolyngbya* from Synechococcales and two species of the genus *Nostoc* from Nostocales order were dominant on monuments and have been recorded from France (Barberousse, 2006). Uher *et al.*, (2005) reported six species of genus *Leptolyngbya* and two species of *Nostoc* from the monuments and building of South Eastern Spain. The monuments at Tikal, Guatemala however had dominance of cyanobacteria belonging to genera *Aphanothece*, *Gloeocapsa*, *Gloeocapsopsis* and *Chroococcus* from the orders Chroococcales (Ortega-Morales *et al.*, 2013). In other past studies genera like *Phormidium* (Ortega-Calvo *et al.*, 1991), *Gloeocapsa*, *Phormidium* and *Chroococcus* (Macedo *et al.*, 2009), *Gloeocapsa* and *Leptolyngbya* (Ramirez M. *et al.*, 2010) have been reported as major species from the biofilm of different monuments of Salamanca, Seville, Toledo Cathedral of Spain and Lund Cathedral of Sweden, monuments of Mediterranean Basin and Mayan archeological sites in Palenque respectively.

5.1.2 Bryophyte

A total of seventeen species of bryophytes were recorded from the study area. This includes sixteen species from the selected monuments of the Champaner-Pavagadh complex and two species from the studied MSU monuments (Table 5.6). It included nine species of

Biodeterioration of Selected Historical Monuments by Lower Plants and Cyanobacteria

liverworts, six species of mosses and two species of hornworts. Among these species, maximum species of liverworts were from the order Marchantiales (*Riccia*, *Plagiochasma*, *Asterella* and *Cyathodium*), mosses from the order Pottiales (*Semibarbulla*, *Hyophila*, *Hydrogonium* and *Gymnostomiella*) and hornworts from the order Anthocerotales (*Anthoceros*).

Table 5.6 – Diversity and distribution of Bryophytes on selected monuments

Sr. No.	Name of the biofoulants	Selected monument sites							
		Champaner Pavagadh						MSU campus	
		1	2	3	4	5	6	7	8
Mosses									
1.	<i>Anomobryum auratum</i> (Mitt.) Jaeg.					+			
2.	<i>Fissidens splachnobryoides</i> Broth. in Schum. et Lauterb.			+		+			
3.	<i>Hydrogonium arcuatum</i> (Griff.) Wijk. et Marg.	+						+	
4.	<i>Hyophila involuta</i> (Hook.) Jaeg.	+	+	+	+	+			
5.	<i>Semibarbulla orientalis</i> (Web.) Wijk et Marg.					+			
6.	<i>Gymnostomiella vernicosa</i> (Hook.) Fleisch.					+		+	+
Liverworts									
7.	<i>Asterella angusta</i> (Steph.) Kachroo.				+	+			
8.	<i>Cyathodium cavernarum</i> Kunze.					+			
9.	<i>Lejeunea aloba</i> Sande Lac.					+			
10.	<i>Riccia gangetica</i> Ahmad.						+		
11.	<i>Riccia discolor</i> L. et L.		+						
12.	<i>Riccia grollei</i> Udar.			+					
13.	<i>Riccia billardieri</i> Mont. et Nees.		+				+		
14.	<i>Plagiochasma microcephalum</i> (Steph.) Steph.					+			
15.	<i>Plagiochasma appendiculatum</i> L. et L.				+	+			
Hornworts									
16.	<i>Anthoceros bhadarwajii</i> Udar et. Asthana						+		
17.	<i>Anthoceros subtilis</i> St.						+		

1. Saher ki Masjid, 2. Mandavi, 3. Amir Manzil, 4. Makai Kothar, 5. Navlakha Kothar, 6. Jain Temple, 7. Arts Dome, 8. D. N. Hall

Based on the above table, maximum diversity of the species (10) was noticed from the Navlakha Kothar followed by Jain Temple. It might be due to less disturbance by tourists and located at the highest elevation as compare to other selected sites. Other than these, three species were noted from the Mandavi, Makai Kothar and Amir Manzil. Remaining sites Saher ki Masjid and selected sites of MSU campus had two to three species reported.

5.1.2.1 Characteristic features of reported Bryophytes species

The characteristics were observed under the microscope during identification of the species from the standard floras. Here, I wrote the characters based on my observations.

Anomobryum auratum (Mitt.) Jaeg. (Pl. 6)

Plants shining green, branched with catkin like branches up to 1.5 cm long densely radiculose below. Leaves 1.3 mm long, cymbiform, ovate-elliptical, densely imbricate to give shoot a cylindrical appearance, apiculate to obtusely rounded, margin entire; costa slender, pale brown, ending well below apex. Upper cells with thickened walls, linear, 62.82 μ m long and 3.49 μ m wide; basal cells thin walled hyaline, rhomboidal, hexagonal to sub-rectangular, 34.9-55.84 μ m long and 13.96-17.45 μ m wide; middle cells 52.35 μ m long and 5.23-6.98 μ m wide. Plant sterile.

Fissidens splachnobryoides Broth. in Schum. et Lauterb. (Pl. 7)

Plants yellowish green to green, closely gregarious. Plants 6-10 mm long, with 6-8 pairs of leaves. Leaves crowded at apex but lax below. Leaves smaller below; leaves 1.78 mm long and 0.42 mm wide; oblong-lanceolate, apex acuminate, margin entire, bordered all around with two rowed limbidium; vaginate laminae nearly 8/5 of total leaf length; dorsal lamina reaching or ending a little above the leaf insertion; nerve brown, ending far below the apex. Leaf cells smooth, transparent, with very thin walls. Apical cells 6.98-10.47 μ m long and wide; middle cells also 6.98-10.47 μ m long and wide, basal cells 6.98-10.47 μ m long and 10.47-13.96 μ m wide. Sterile plant.

Hydrogonium arcuatum (Griff.) Wijk. et. Marg. (Pl. 8)

Plants yellowish green, more or less stiff tufts. Plants up to 1 cm long, unbranched. Leaves concave, 1.5 to 2 mm long and 0.4 to 0.5 mm broad. Margin entire. Leaf tip acute, pointed, having one or two denticulations at the extreme apex. Costa prominent, yellow brown, percurrent. All leaf cells usually smooth. Apical sub-quadrangle cell 14.31-19.08 μ m long and wide. Middle cells 19.08 – 23.85 μ m long and 14.31- 19.08 μ m wide; lower cells 33.39 – 38.16 μ m long and 14.31 – 19.08 μ m wide. Plant sterile.

Hyophila involuta (Hook.) Jaeg. (Pl. 9)

Plant habit length 9 mm, Stem covered with erect, spreading leaves, leaves oblong in shape, lower oblong part pale, having sheath and toothed above with acute apex. Leaves also having

Biodeterioration of Selected Historical Monuments by Lower Plants and Cyanobacteria

ligule. Costa ending below the apex. Apical and middle cells of leaf round or quadrate hexagonal having papillose. Apical cells 15.23 - 19.08 μm long and wide, middle cells 14.31 – 19.88 μm long and wide, basal cells 32.43- 38.16 μm long and 14.31 - 18.83 μm wide. Seta apical and erect, 2mm long, reddish brown. Capsule erect, cylindrical. Spores and peristome teeth absent.

***Semibarbula orientalis* (Web.) Wijk et Marg. (Pl. 10)**

Plants yellowish green to green. Habit 8 mm long grow densely tufts. Leaves become curled when dry, 1 mm long linear lanceolate, narrower toward apex and broader at base, densely papillose. Costa strong, ending below the apex. Leaf cells sub-quadrate or round sized 9.54 μm long and wide but in lower cells sized on an average 14.34 μm long and 8.34 μm wide. Plant sterile.

***Gymnostomiella vernicosa* (Hook.) Fleisch. (Pl. 11)**

Plants 7-10 mm in length. Stem radiculose, filiform. Leaves distant below but crowded at apex, lower leaves minute, middle and upper leaves large crumpled and appressed in dry condition. Leaf shape oblong, spatulate, concave, margin entire. Upper and middle cells of leaf quadrate 40 -45 μm long and 30-40 μm wide and basal cells rectangular 80 – 90 μm long 30 – 40 μm wide. Plant sterile.

***Asterella angusta* (Steph.) Kachroo. (Pl. 12)**

Thallus prostrate, light green, forming regular and irregular rosettes or overlapping in dense green patches. Thallus dichotomously branched. Ventral scales in two rows, violet and prominent at apex. Scales at the base of carpocephalum and scales end in mucilaginous papillae. Rhizoids tuberculate smooth walled and usually arising from ventral midrib. Male and female plants grow usually in mixed or separately. Female receptacles hemispherical or disc form, stalked, terminal, usually four lobed sometimes 2,3 or even 8 lobed.

***Cyathodium cavernarum* Kunze. (Pl. 13)**

Thallus green or pale green in colour, delicate, small up to 7 mm long and 4-5 mm wide, dichotomously branched. Midrib absent. Spores blackish brown, 30 – 50 μm in diameter, isopolar, spinate. Elaters reddish brown, bispiral or trispiral, 320-450 μm in length and 14-18 μm in width.

Biodeterioration of Selected Historical Monuments by Lower Plants and Cyanobacteria

***Lejeunea aloba* Sande Lac. (Pl. 14)**

Plants 2 cm long irregularly branched, flaccid, yellowish green. Leaves imbricate one cell thick horizontally spread, broad ovate, 0.7 mm broad and 0.8 mm long inserted by a short stalk, apex broad and round. amphigastria large, broader than stem, bifid, sinus narrow, lobes triangular. Rhizoids unicellular and smooth. Plant sterile.

***Riccia gangetica* Ahmad. (Pl. 15)**

Plants bluish green, overlapping in patches or forming well defined rosettes. Thallus 5 mm long and 2 mm broad, dichotomous branched, lobes ovate, dorsal median groove prominent. Rhizoids dense, simple and tuberculated. Scale hyaline or purple. Monoecious. Sterile plant.

***Riccia discolor* L. rt L. (Pl. 16)**

Plants overlapping in dense patches very rarely form irregular rosettes. Thallus green, once or twice forked and oblong lobes. Thallus up to 7 mm long and 2.5 mm wide. Groove is narrow at apex and then flat all along the length. Plant sterile.

***Riccia grollei* Udar. (Pl. 17)**

Plants bluish green, simple or once forked, thallus 5-6 mm long and 2-3 mm broad, dorsally sulcate. Scales large, purple evidently extending beyond the margins. Monoecious. Sterile plant.

***Riccia billardieri* Mont. et Nees. (Pl. 18)**

Thallus pale green to dark or bluish green, usually overlapping, forming dense patches and sometimes forming irregular rosettes. Thallus simple or dichotomously branched and up to 20 mm long and up to 10 mm broad. Scale purple, sparse and widely separated not extending beyond the margins. Rhizoids smooth walled and tuberculated, Plant sterile.

***Plagiochasma microcephalum* (Steph.) Steph. (Pl. 19)**

Thallus upto 20 mm long, 3-6 mm wide, bright green, border wide with violet margin. Scales in 1-2 rows, violet, cells pink or hyaline. Male receptacle rounded or reniform situated in the median part of thallus rarely at the base of articulation. Female receptacle situated in median part of thallus, very rarely at the base of articulation.

Biodeterioration of Selected Historical Monuments by Lower Plants and Cyanobacteria

***Plagiochasma appendiculatum* L. et L. (Pl. 19)**

Thallus green, large dense patches, usually 10 – 20 mm long upto 10 mm wide. Dichotomous branched, lobes long, smooth dorsal surface. Antheridia club shaped, developed acropetally in each lobe. Male receptacles born in groups or behind the female receptacle or the receptacle born one after other. Female receptacle sessile or short stalked usually without rhizoidal furrow, 2 to 3 lobed. Monoecious.

***Anthoceros bhadarwajii* Udar et. Asthana (Pl. 20)**

Thallus 9 mm long and 14-16 mm wide at fanning apex. Spores dark brown, 45.20 µm in diameter with spinulate blunt projections forming reticuloid pattern, proximal faces marked with distinct triradiate rays.

***Anthoceros subtilis* St. (Pl. 21)**

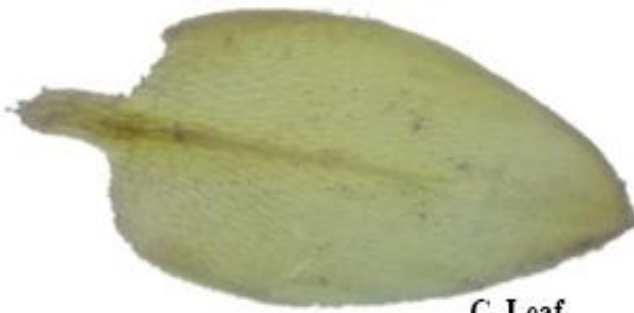
Thallus forming rosettes of 8 mm. Spores brown in colour having diameter 39.42 - 42.12 µm with spinulate – laculate projections. Elaters light brown in colour having dark thin bands on it, thin walled 134 µm long, complete elaters having 4 celled.



A. Habitat



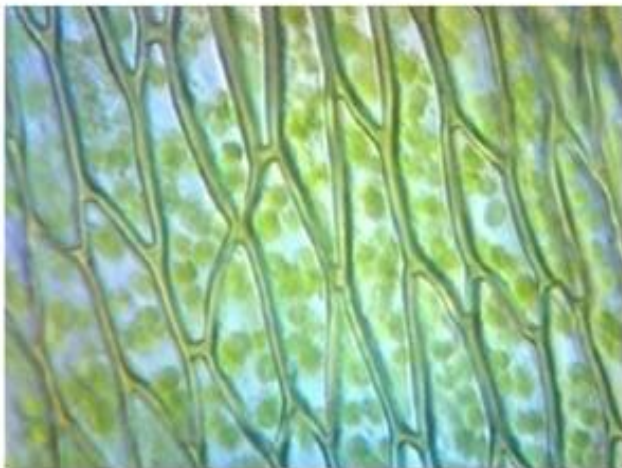
B. Habit



C. Leaf



D. Enlarge view of
leaves arrangement



E. Cells of the leaf part

Scale bars

B. ————— 2 mm

C. ————— 0.5 mm

D. ————— 1 mm

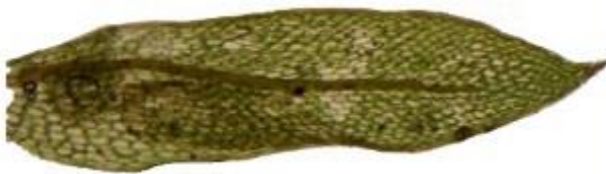
E. ————— 0.1 mm



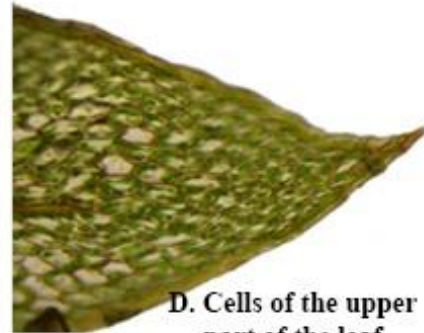
A. Habitat



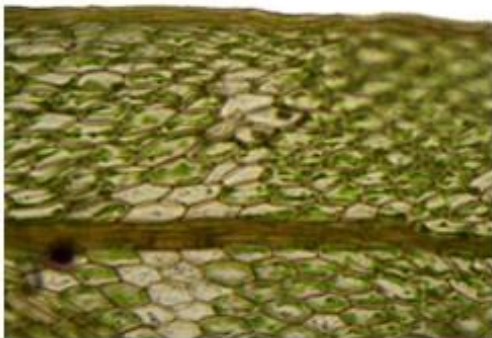
B. Habit



C. Leaf



D. Cells of the upper part of the leaf



E. Cells of the middle part of the leaf

F. Cells of the lower part of the leaf



Scale bars

B. _____ 2 mm

C. _____ 0.5 mm

D. _____ 0.1 mm

E. _____ 0.1 mm

F. _____ 0.1 mm

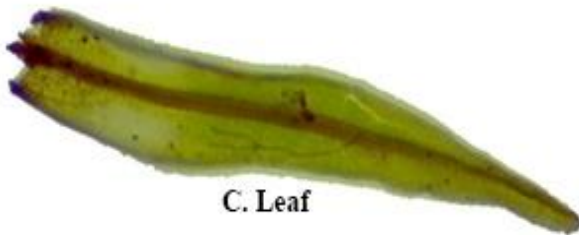
Plate 7 – *Fissidens splachnobryoides* Broth. in Schum. Et Lauterb.



A. Habitat



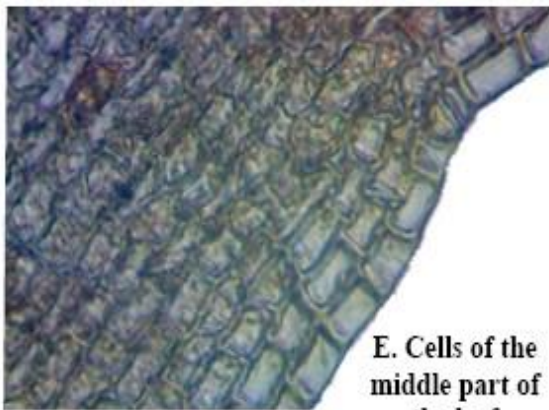
B. Habit



C. Leaf



D. Cells of the upper part of the leaf



E. Cells of the middle part of the leaf



F. Cells of the lower part of the leaf

Scale bars

B. _____ 4 mm

C. _____ 1 mm

D. _____ 0.1 mm

E. _____ 0.1 mm

F. _____ 0.05 mm



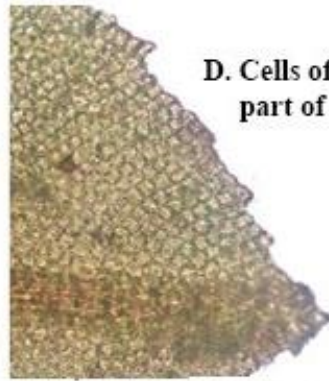
A. Habitat



B. Habit



C. Leaf



D. Cells of the upper part of the leaf



E. Cells of the middle part of the leaf



F. Cells of the lower part of the leaf

Scale bars

B. _____ 2 mm

C. _____ 1 mm

D. _____ 0.04 mm

E. _____ 0.04 mm

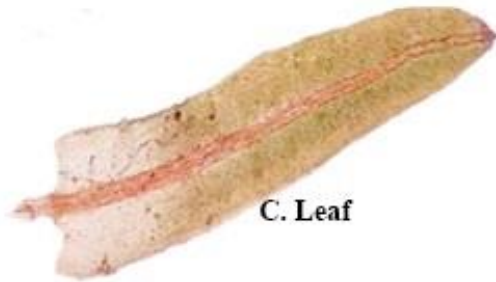
F. _____ 0.04 mm



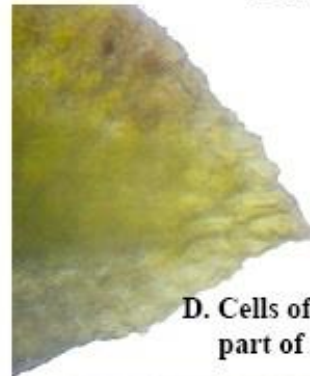
A. Habitat



B. Habit



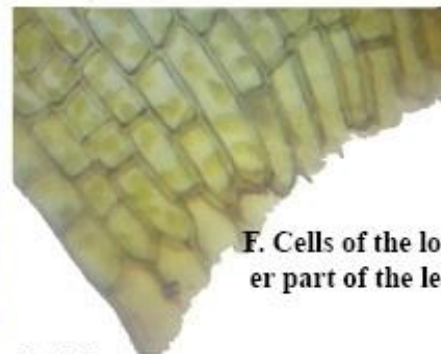
C. Leaf



D. Cells of the upper part of the leaf



E. Cells of the middle part of the leaf



F. Cells of the lower part of the leaf

Scale bars

B. _____ 4 mm

C. _____ 0.5 mm

D. _____ 0.05 mm

E. _____ 0.05 mm

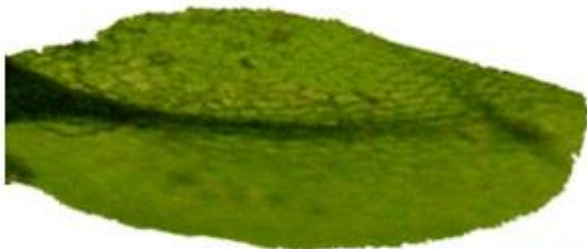
F. _____ 0.05 mm



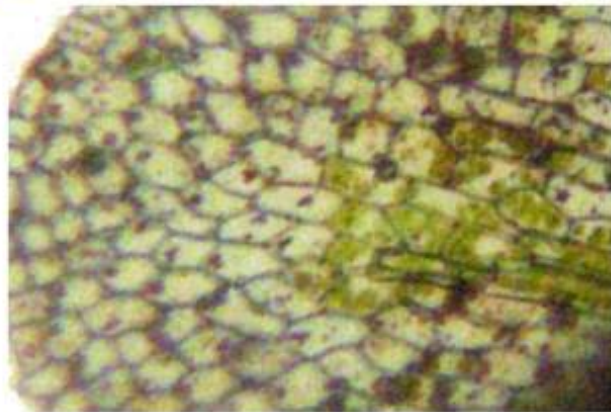
A. Habitat



B. Habit



C. Leaf



D. Cells of the leaf part

Scale bars

B.  2 mm

C.  1 mm

D.  0.1 mm

Plate 11 – *Gymnostomiella vernicosa* (Hook.) Fleisch.



A. Habitat



B. Habit



C. Ventral surface showing scale



D. Female receptacle
with five lobes

Scale bars

B.  4 mm

D.  2 mm

Plate 12 – *Asterella angusta* (Steph.) Kachroo.



A. Habitat



B. Habit



C. Spore



D. Eleter

Scale bar

B. _____ 4 mm

C. _____ 0.1 mm

D. _____ 0.1 mm

Plate 13 – *Cyathodium cavernarum* Kunze.



A. Habitat



B. Habit



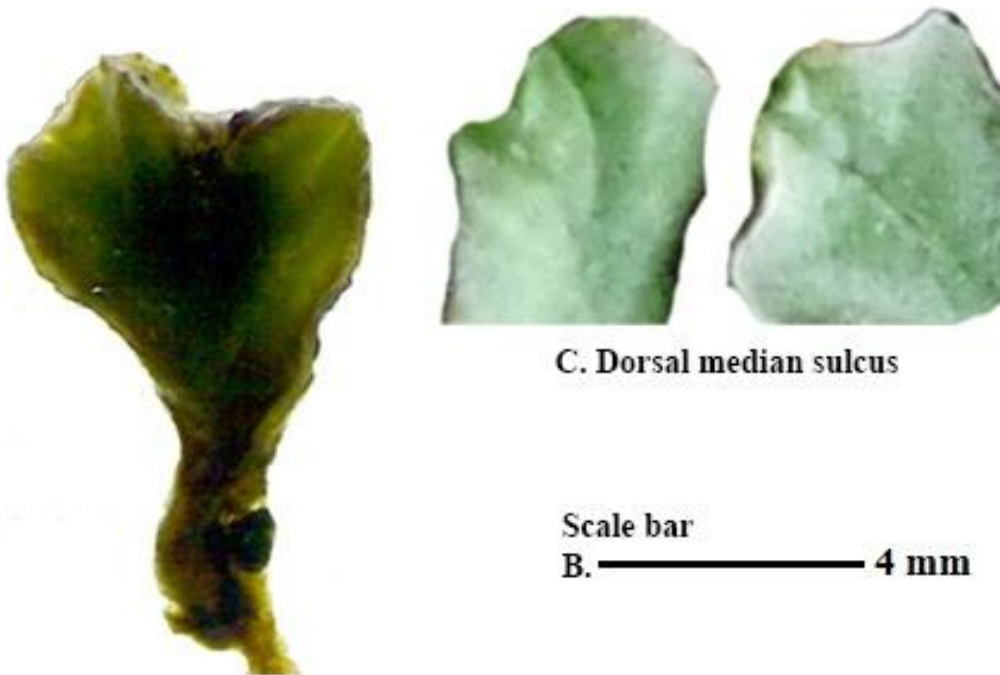
C. Ventral surface showing leaf arrangement

Scale bar

B. ————— 4 mm



A. Habitat



B. Habit

C. Dorsal median sulcus

Scale bar
B. ————— 4 mm



A. Habitat



B. Habit



C. Ventral surface showing scale

Scale bar

B., C.  5 mm

Plate 16 – *Riccia discolour* L.r.t. L.



A. Habitat



B. Habit



C. Ventral surface showing scale

Scale bar
B., C. ————— 5 mm

Plate 17 – *Riccia grollei* Udar.



A. Habitat



B. Habit



C. Ventral surface showing scale

Scale bar

B., C.  5 mm



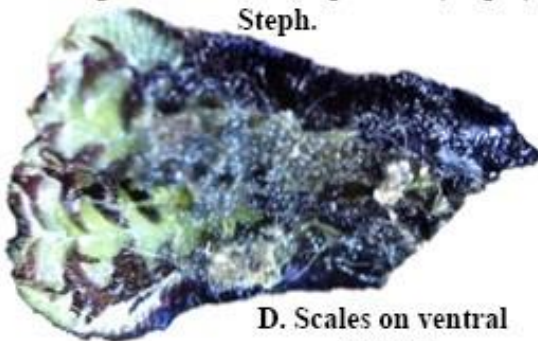
A. Habitat of *Plagiochasma microcephalum* and *Plagiochasma appendiculatum* mixed population



B. *Plagiochasma microcephalum* (Steph.)
Steph.



C. *Plagiochasma appendiculatum*



D. Scales on ventral surface

Scale bars

B. _____ 5 mm

C. _____ 5 mm



A. Habitat



B. Habit



C. Columela



D. Spore

Scale bars

B.  5 mm

C.  2 mm

D.  0.1 mm



A. Habitat



B. Habit



C. Columela



D. Eleter



E. Spore

Scale bars

B. _____ 5 mm

C. _____ 2 mm

D., E. _____ 0.1 mm

5.1.2.2 Status of Bryophytes on the monuments

Total seventeen species of bryophytes were found from the selected study locations. Species of the order Marchantiales followed by members of order Pottiales were dominant on the monuments of the Champaner-Pavagadh. From the order Marchantiales, *Riccia* was the most common genera followed by *Plagiochasma*, *Asterella* and *Cyathodium*. Species from the order Marchantiales such as *Plagiochasma*, *Marchantia* and *Asterella* were also been recorded on the monuments of Talala Ghar, Assam (Verma *et al.*, 2014). Several genera of the Pottiales viz. *Semibarbula*, *Hyophila*, *Hydrogonium* and *Gymnostomiella* followed by *Fissidens* from the order Dicranales and *Anomobryum* from the order Bryales were found during the current study. The genus *Hyophila* and *Gymnostomiella* are considered to be arid mosses and have been reported from a few monuments in Gujarat. (Shah and Gujar, 2015). However, there are few other reports about the presence of members of Pottiales from other monuments. Members of Funariales like *Funaria* and *Phsicomatrium* from the Tala Ghar, Assam (Verma *et al.*, 2014) and *Funariella curviseta* and *Entosthodon pulchellus* from the archaeological sites of Chellah, Moroco (Elharech *et al.*, 2017) have been reported by past workers. An unidentified species of *Fissidens* and *Fissidens bryoides* which are members of the order Dicranales have been reported from the monuments of Talala Ghar (Assam) and the archaeological site of Chellah, Morocco respectively (Verma *et al.*, 2014; Elharech *et al.*, 2017). In the current study, the leafy liverwort *Lejeunea aloba* of the Porellales order was also reported. It was observed growing on wall of the Navlakhi Kothar. This particular species has generally been reported to grow epiphytically on trees and shrubs but has not been reported to grow on buildings. This represents an exceptional habitat for *Lejeunea aloba*. *Anomobryum auratum* from the order Bryales were found growing in crevices of the rocks which were exposed to the elements. Other past studies (Elharech *et al.*, 2017) have reported the presence of other members of the order bryales viz., *Plychostomum capillare* and *Bryum radiculosum* from the archaeological site of Chellah, Morocco. Most of the studies cited here as well in the review of literature showed the dominance of mosses on the monuments, but in the current study, liverworts dominated over the mosses.

5.1.3 Lichen

A total of 8 lichen species could be identified during the study. They included four crustose lichens (*Caloplaca awasthii*, *C. cuplifera*, *Pertusaria multipunta* and *Diploschistes* sp.), two crustose to leprose lichens (*Lepraria caresnsri*, *L. lobificans*), one squamulose lichen (*Endocarpon nanum*) and one foliose lichen (*Phaeophysia hispidula*). All lichen

Biodeterioration of Selected Historical Monuments by Lower Plants and Cyanobacteria

samples were deposited in the NBRI herbarium repository and their accession numbers were obtained. The field book numbers and the accession numbers of these species are mentioned in Table. 5.7 below. The distribution of all the species are given in Table 5.8. No lichen species were found on the monuments of the MSU campus and monuments of the Champaner at the foothill of Pavagadh.

Table 5.7 – Field book numbers and accession numbers of lichen samples

Sr. No.	Species Name	Field Book No.	Accession No.
1.	<i>Caloplaca awasthii</i> Y. Joshi & Upreti	19-038033	42454
2.	<i>Caloplaca cupulifera</i> (Vain.) Zahlbr.	19-038034	42458
3.	<i>Pertusaria multipuncta</i> (Turner) Nyl.	20-038029	42457
		20-038030	42456
4.	<i>Diploschistes</i> Norman	20-038028	42453
5.	<i>Lepraria coriensis</i> (Hue) Sipman	19-038036	42460
6.	<i>Lepraria lobificans</i> Nyl.	19-038035	42459
7.	<i>Endocarpon nanum</i> Ajay Singh & Upreti	20-038027	42452
8.	<i>Phaeophyscia hispidula</i> (Ach.) Essl.	20-038031	42462
		20-038032	42461

Table 5.8 – Diversity and distribution of Lichens on selected monuments

Sr. No.	Name of the biofoulants	Selected monument sites							
		Champaner Pavagadh						MSU campus	
		1	2	3	4	5	6	7	8
Lichen									
1.	<i>Caloplaca awasthii</i> Y. Joshi & Upreti					+			
2.	<i>Caloplaca cupulifera</i> (Vain.) Zahlbr.				+				
3.	<i>Pertusaria multipuncta</i> (Turner) Nyl.					+	+		
4.	<i>Diploschistes</i> Norman					+			
5.	<i>Lepraria coriensis</i> (Hue) Sipman						+		
6.	<i>Lepraria lobificans</i> Nyl.					+			

Biodeterioration of Selected Historical Monuments by Lower Plants and Cyanobacteria

7.	<i>Endocarpon nanum</i> Ajay Singh & Upreti					+			
8.	<i>Phaeophyscia hispidula</i> (Ach.) Essl.					+	+		

1. Saher ki Masjid, 2. Mandavi, 3. Amir Manzil, 4. Makai Kothar, 5. Navlakha Kothar, 6. Jain Temple, 7. Arts Dome, 8. D. N. Hall

5.1.3.1 Characteristics of Lichens

The key characteristics observed under microscope have been described below. Identification was carried out by observing characters and chemical spot test from the standard references mentioned in the chapter 4.

***Caloplaca awasthii* Y. Joshi & Upreti (Pl. 22)**

Thallus crustose, smooth, glossy, effigurate to subsquamulose, central portion lobed to areolate, yellow orange. Lobes irregularly branched, plane to subconvex, tightly appressed to substratum, regular to flabellate, marginal lobes 1.0 – 1.5 mm long and 0.5 – 1.0 mm wide. Medulla white composed of loosely arranged hyphae. Prothallus, Apothecia and pycnidia absent. Thallus K+ purple, C-, KC-, P-

***Caloplaca cupulifera* (Vain.) Zahlbr. (Pl. 23)**

Thallus crustose, areolate, bright, orange to deep yellow chrome. Lobes marginal areoles, margin thinning, lobes 0.2 – 0.4 mm long and 0.2 – 0.3 mm wide. Sorediate, soralia small, crateriform, soredia granular, concolorous or paler than thallus. Prothallus, Apothecia and pycnidia absent. Thallus K+ purple, C-, KC-, P-

***Pertusaria multipuncta* (Turner) Nyl. (Pl. 24)**

Thallus crustose, granular or verrucose, fissured or areolate, sorediate. Apothecia generally elevated and innate in fertile verruca, rarely present, disc becoming sorediose, 1-4 apothecia per verruca. Thallus K-, P-, C-, KC-.

***Diploschistes* Norman (Pl. 25)**

Thallus crustose, uniform or verrucose, ecorticated or with a corticiform layer, saxicolous. Apothecia was absent, hence species level identity was not confirmed yet.

Biodeterioration of Selected Historical Monuments by Lower Plants and Cyanobacteria

***Lepraria coriensis* (Hue) Sipman (Pl. 26)**

Thallus leprose, powdery to membranous, margin delimited, lobes present, obscure or more often well develop 1-2 mm diameter and raised marginal rim. Medulla white in colour. Soredia fine to coarse, up to 300 µm diameter. Projecting hyphae absent. Thallus K-, KC-, C-, P-.

***Lepraria lobificans* Nyl. (Pl. 27)**

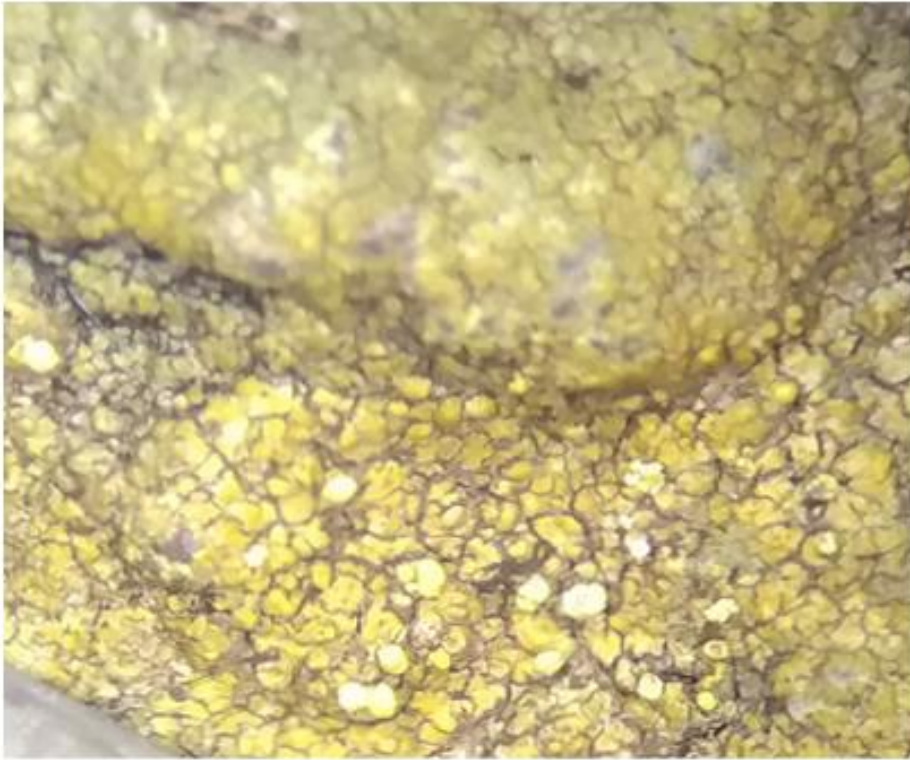
Thallus leprose, soft, light green to light grey colour, cottony to powdery, medulla present, soredia loosely packed, abundant, vary in size up to 60 diameters. Projecting hyphae present. Thallus K+ yellow, C-, KC-, Pd+ orange.

***Endocarpon nanum* Ajay Singh & Upreti (Pl. 28)**

Thallus squamulose, up to 1 cm across, squamules plane to slightly concave, adnate, round to irregular in outline, greenish grey in wet condition but yellowish brown in dry condition. Lower surface of squamuloses pale white to yellow brown, one perithecium per squamule, ostiole protruding with black rimmed. Thallus K-, KC-, C-, P-.

***Phaeophyscia hispidula* (Ach.) Essl. (Pl. 29)**

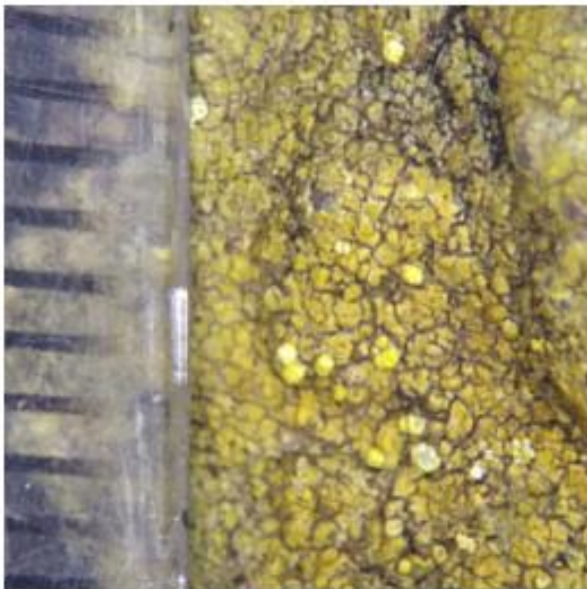
Thallus foliose, ashy white to grey, loosely attached to the substratum, growing in sub orbicular patches, lobate. Lobes up to 4 mm long irregularly branched, discrete or imbricate, border concave at the ends. Epruinose, sorediate, soredia laminal. Medulla white in colour. Lower surface underside black with long black rhizines which projecting beyond the margins. Apothecia absent. Thallus K-, C-, KC-, P-.



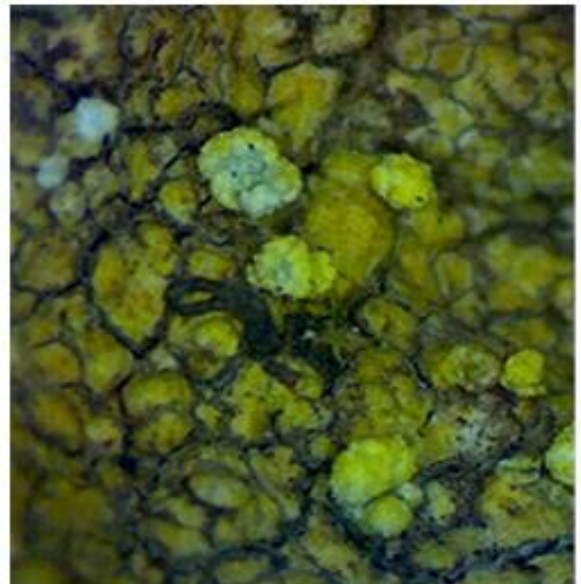
A. Habitat



D. Chemical spot test result



B. Habit with scale



C. Close up view of thallus

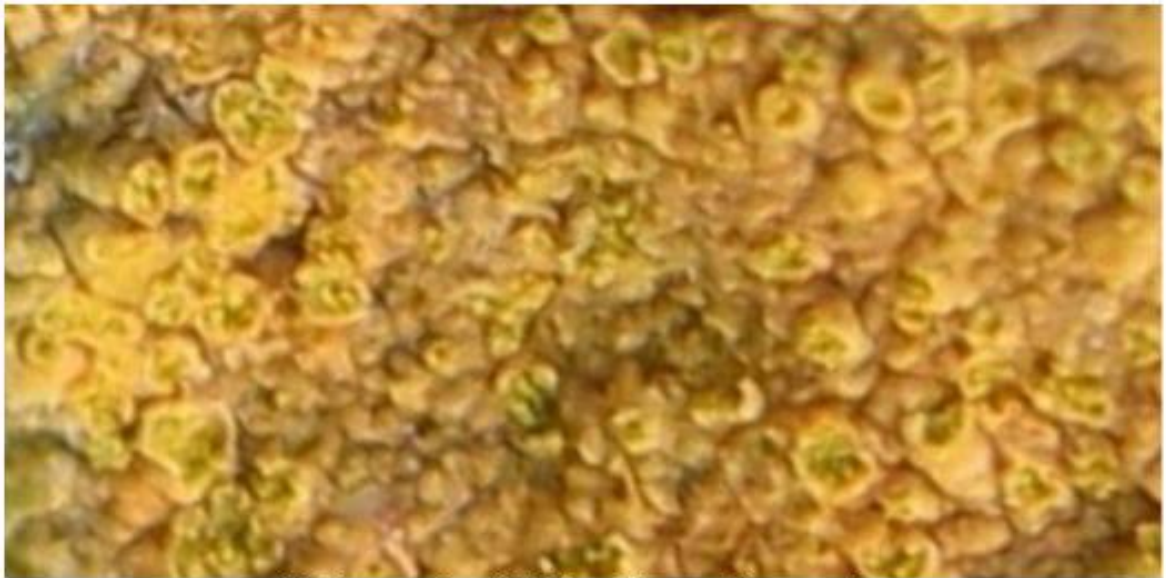
Plate 22 – *Caloplaca awasthii* Y. Joshi & Upreti



A. Habitat



C. Chemical spot test result



B. Close up view of thallus with crateriform soralia

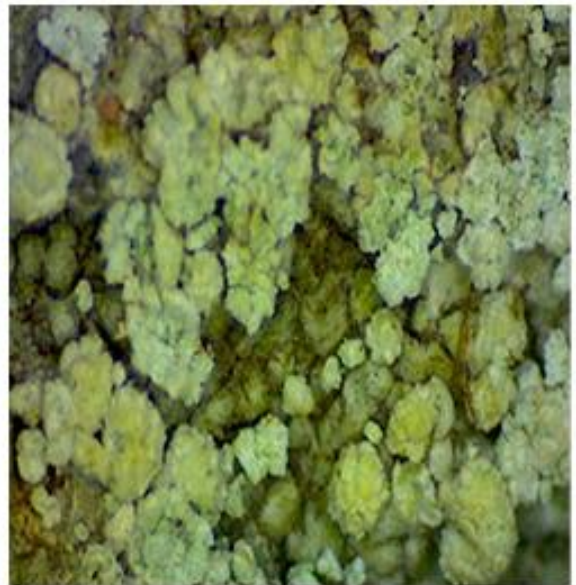
Plate 23 – *Caloplaca cupulifera* (Vain.) Zahlbr.



A. Habitat



B. Habit with scale



C. Close up view of thallus with soredia

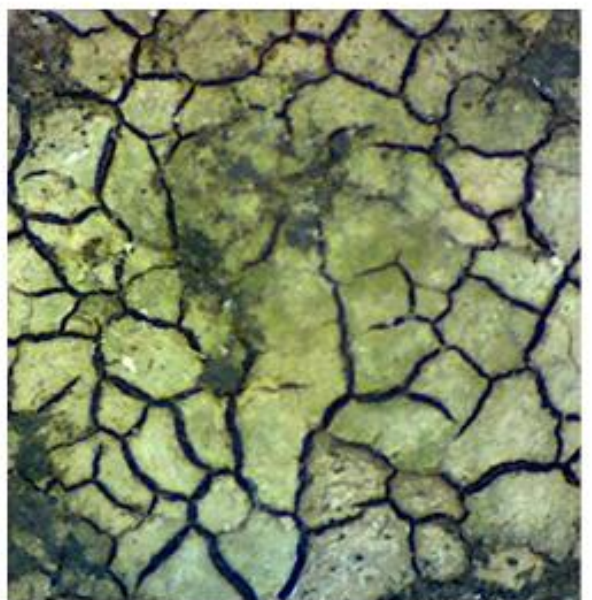
Plate 24 – *Pertusaria multipuncta* (Turner) Nyl.



A. Habitat



B. Habit with scale



C. Close up view of thallus

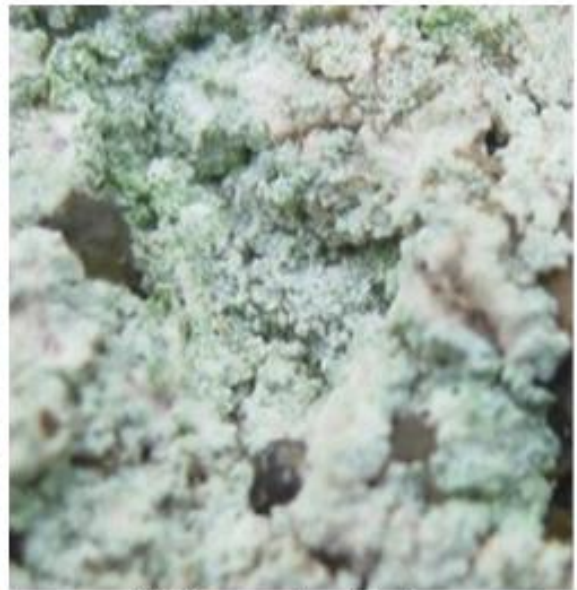
Plate 25 – *Diploschistes* Norman



A. Habitat



B. Habit with scale



C. Close up view of thallus

Plate 26 – *Lepraria coriensis* (Hue) Sipman



A. Habitat



B. Close up view of thallus with soredia

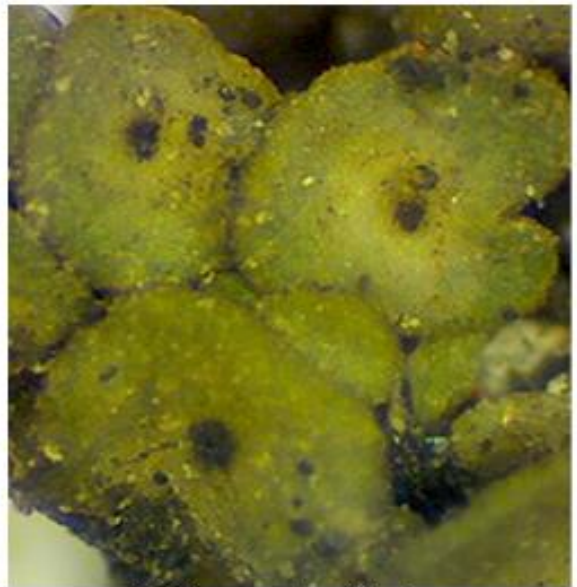
Plate 27 – *Lepraria lobificans* Nyl.



A. Habitat



B. Habit with scale



C. Close up view of thallus



A. Habitat



B. Habit with scale



C. Projection of Black Rhizines beyond margin

Plate 29 – *Phaeophyscia hispidula* (Ach.) Essl.

5.1.3.2 Status of Lichens on monuments

In current study, the crustose lichens were the dominant lichen form on the selected monuments. Two species of leprose lichens and one species each of squamulose and foliose lichens were found from the selected study sites. Six species viz., *Caloplaca awasthii*, *Diploschistes* sp., *Lepraria lobificans*, *Endocarpon nanum* were recorded from a single monument, the Navlakha Kothar. *Lepraria coriensis* and *Caloplaca cupilifera* were found from the Jain temple and Makai Kothar respectively. Both *Pertusaria multipuncta* and *Phaeophyscia hispidula*, were dominant on the antiquity surrounding the Jain temple and the Navlakha Kothar. Similar results by Joshi *et al.*, (2015) reported crustose lichen genus *Caloplaca*, foliose lichen genus *Phaeophyscia* and leprose lichen genus *Lepraria* from the Jageshwar monuments, Uttarakhand. Likewise, two species of *Caloplaca* was also recorded from the historical Bamuni hill of Assam (Choudhury *et al.*, 2016). Uppadhyay *et al.*, (2016) reported squamulose form of lichen that included two species of genus *Endocarpon* as dominant species from the monuments in and around Gwalior. Nayaka *et al.*, (2017) recorded maximum number of crustose lichens and of which genus *Caloplaca* was predominant from the Konark sun temple. The current study having similar four genera namely *Caloplaca*, *Diploschistes*, *Pertusaria* and *Lepraria* were recorded from the Sun temple of Konark (Nayaka *et al.*, 2017). Same as current study, Bajpai and Upreti, (2014) documented similar species of lichens namely *Endocarpon nanum* from the various monuments from the Karnataka, Madhya Pradesh, Maharashtra, Orissa and Utter Pradesh while *Lepraria lobificans* and *Caloplaca* sp. were reported from the monuments of Madhya Pradesh, Maharashtra and Utter Pradesh. With the exception of *Pertusaria multipuncta* and *Lepraria coriensis* most of the other species discovered in the current study have been recorded from monuments in India (Bajpai and Upreti, 2014; Choudhury *et al.*, 2016; Nayaka *et al.*, 2017).

Broadly lichen species on the monuments of Europe and Netherlands did not had any similarity with current study of diversity of lichens, except genus *Caloplaca* (Aptroot and James, 2002; Bultmann *et al.*, 2015; Aptroot *et al.*, 2017).

5.1.4 Geological Investigation

The mineral composition of the collected four geological samples were studied by thin sections of the rocks samples and Powder X-ray Diffraction (XRD) analysis. The study revealed the presence of mainly primary and secondary silica, ferruginous materials, calcareous material and feldspar minerals.

5.1.4.1 Thin section of rock samples

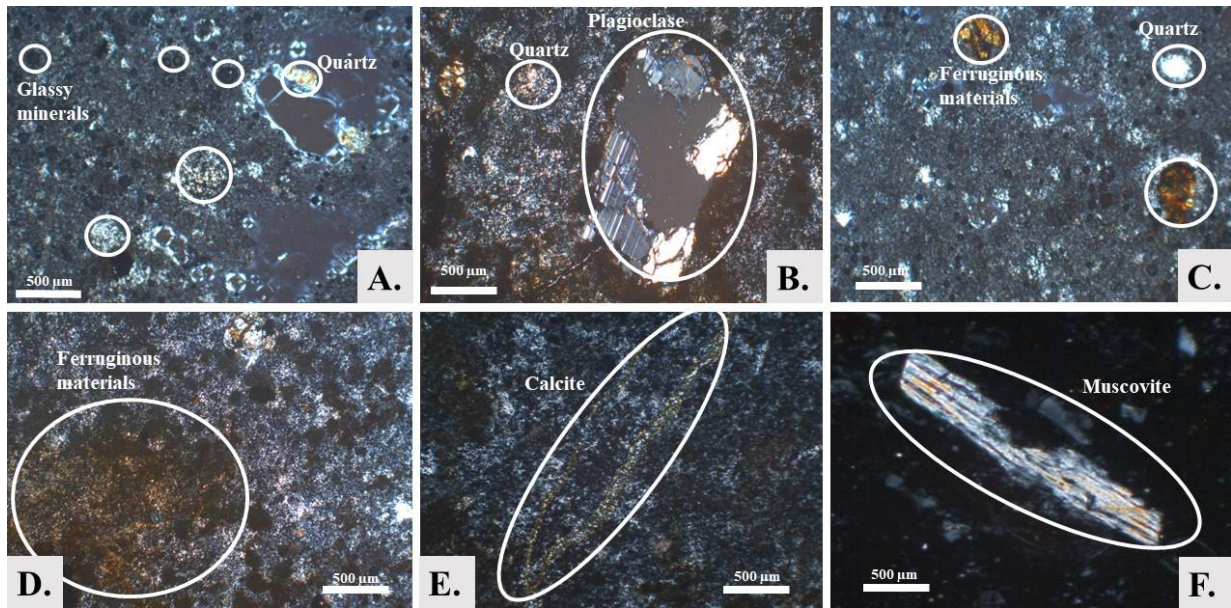


Fig. 5.6 – Microscopic photographs of samples thin section of different sites
A., B., C. – Makai Kothar D., E., F. – Jain Temple

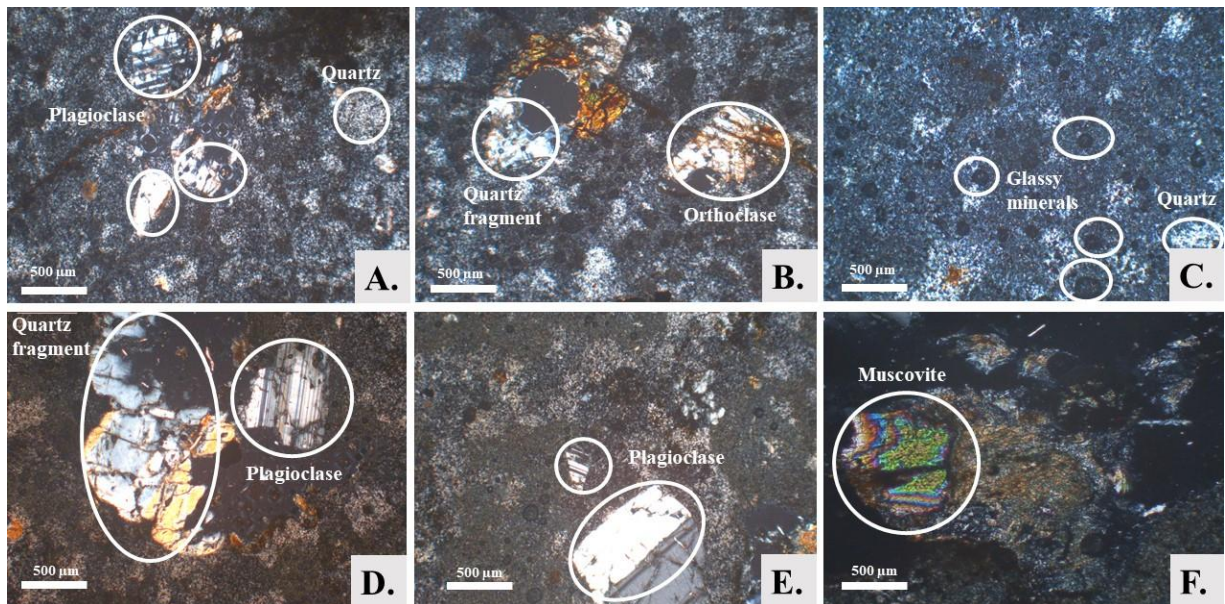


Fig. 5.7 – Microscopic photographs of samples thin section of different sites
A., B., C. - Antiquity from surrounding the Jain Temple D., E., F. – Navlakha Kothar

The microscopic analysis of the thin sections showed the presence of different minerals scattered at different sites within the ground mass. Fig. 5.6 and 5.7 depict characteristic mineral images found within the four different samples analysed. As the images of both plates show, the ground mass is majorly composed of primary and secondary silica as

Biodeterioration of Selected Historical Monuments by Lower Plants and Cyanobacteria

well as glassy minerals. Glassy minerals are obtained from the pyroclastic rock. Pyroclastic rock is an igneous rock which is formed through volcanic eruption. Volcanic clastic is deposited predominantly as volcanic particles. These glassy minerals have composition of siliceous materials. Quartz was also observed surrounded by this siliceous material. Image B in fig. 5.6 and images A, D and E of fig. 5.7, showed fragments of Plagioclase minerals with siliceous ground mass. Plagioclase minerals are within the feldspar group and are produced by weathering of igneous and metamorphic rock. Chemical composition of plagioclase consists of calcium or sodium elements containing siliceous materials (silicates). It appears light in colour, glassy, transparent to translucent with striations. The orange to brown patches observed in a few of the images are deposited material known as ferruginous minerals of iron oxide. In fig. 5.7 image B, crystals having colourless or light colour (white or grey) are of orthoclase. Orthoclase belongs to the feldspar group. Its chemical composition is potassium with silicate minerals. Hence, orthoclase also known as K-feldspar or Microcline. Images F of fig. 5.6 and 5.7, show muscovite, a mineral rich of potassium, iron and magnesium elements. It appears white to colourless, silvery-white and tinged by various colours due to impurities. It belongs to the Mica family. The strips-like structure observed in Image E of fig.

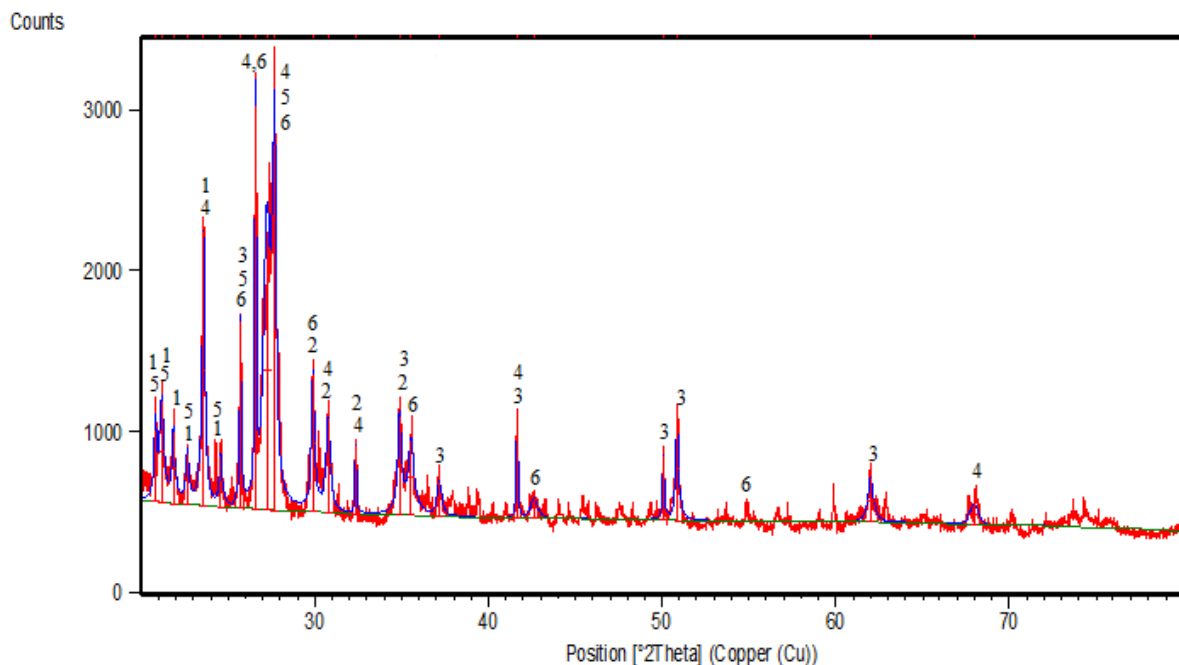


Fig. 5.8 – XRD spectra of rock sample of Makai Kothar

1. Aluminosilicate, 2. Calcite, 3. Orthoclase, 4. Plagioclase, 5. Muscovite, 6. Hematite and Magnetite

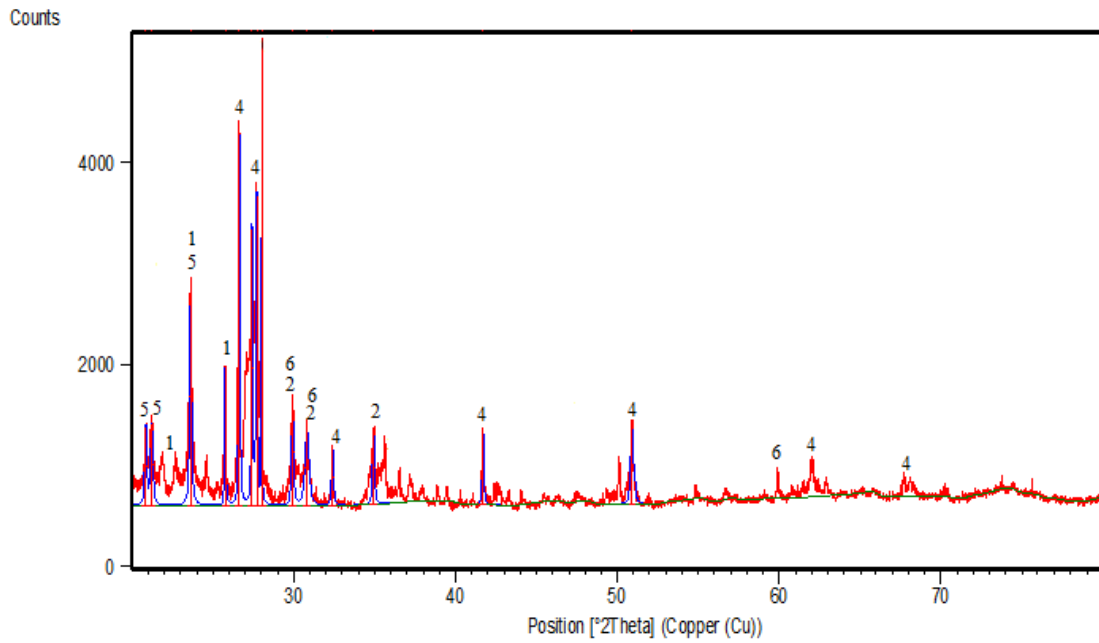


Fig. 5.9 – XRD spectra of rock sample of Jain temple

1. Aluminosilicate, 2. Calcite, 3. Orthoclase, 4. Plagioclase, 5. Muscovite, 6. Hematite and Magnetite

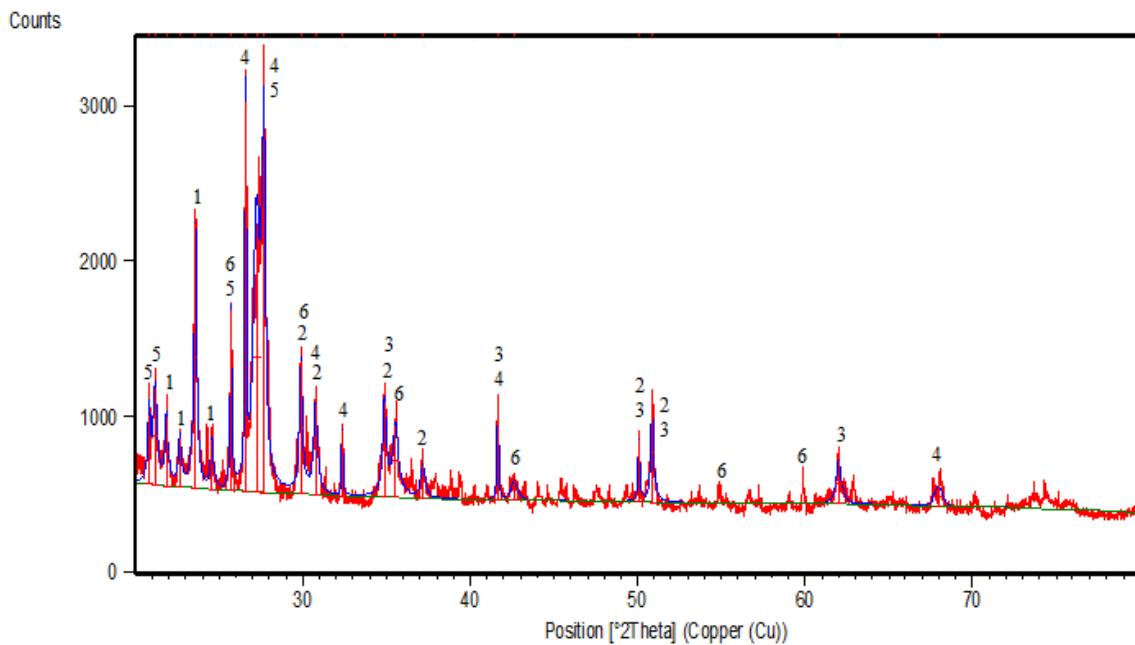


Fig. 5.10 – XRD spectra of rock sample of antiquities from surrounding the Jain temple

1. Aluminosilicate, 2. Calcite, 3. Orthoclase, 4. Plagioclase, 5. Muscovite, 6. Hematite and Magnetite

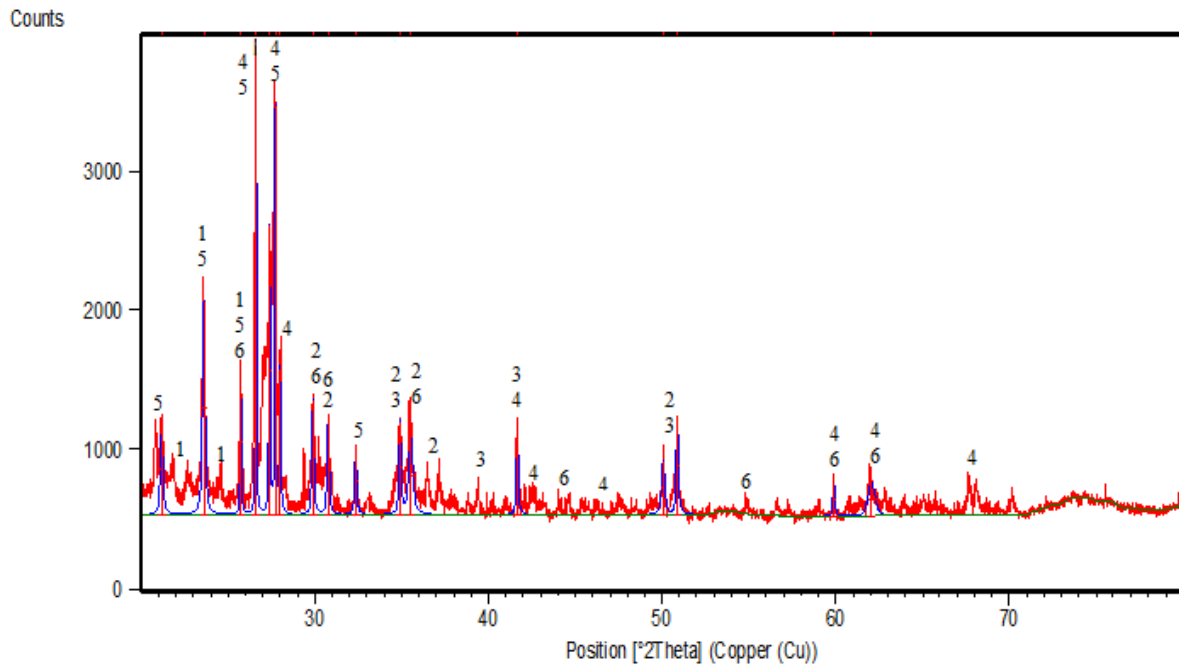


Fig. 5.11 – XRD spectra of rock sample of Navlakaha Kothar

1. Aluminosilicate, 2. Calcite, 3. Orthoclase, 4. Plagioclase, 5. Muscovite, 6. Hematite and Magnetite

5.6, is made up of calcite mineral. It is a carbonate mineral and is very commonly found in igneous, metamorphic and sedimentary rocks.

5.1.4.2 XRD analysis of rock samples

The powder XRD analysis of the rock samples was carried out to obtain information on the major mineral components of the sample. The figures 5.8 to 5.11 below depict the spectra obtained for the different samples.

In powder X-ray diffraction spectra depicted above, the 2θ peak appear at 6.7, 8.75, 9.04, 12.12, 24.318 which corresponds to planes of lower miller indices like (0 1 0), (0 0 1), (1 0 0), (1 0 0), (0 0 1) and are characteristics of mineral from Mica categories like muscovite. The diffraction peaks at 9.38°, 12.90° and 17.2° are due to diffraction from (0 1 0), ($\bar{1}$ 1 0) and (1 1 1) planes respectively. This indicates the presence of Aluminosilicate minerals which may have the chemical formula is $\text{Ca}_2\text{Al}_4\text{Si}_8\text{O}_{24}$ (JCPDS card number PDF # 861548). The 2θ peak at 29.37°, 31.39°, 35.93° and 39.37° are due to diffraction from (1 0 4), (0 0 6), (1 1 0) and (1 1 3) planes respectively. These peaks have characteristic diffraction due to calcite minerals which have chemical formula CaCO_3 (JCPDS card number PDF # 721937).

Biodeterioration of Selected Historical Monuments by Lower Plants and Cyanobacteria

The diffraction peak at 28.62°, 34.73°, 41.51°, 51.60° and 62.26° are due to diffraction from (1 0 2), (1 1 0), (0 0 4), (2 0 3) and (3 0 0) planes respectively due to Potassium aluminosilicate which may have chemical formula $KAlSiO_4$ (JCPDS card number # 851413). Potassium aluminosilicate is K-feldspar. The peaks at higher angles like 31.5, 36.23, 44.5, 54.25, 60.5 and 65.25 are due to diffraction from (2 2 0), (3 1 1), (4 0 0), (4 2 2), (5 1 1) and (4 4 0) respectively. These peaks are due to iron oxide containing minerals like Hematite (Fe_2O_3) and Magnetite (Fe_3O_4). The major peaks at 20.86°, 26.64°, 42.45°, 50.15°, 50.63°, 59.97°, 68.15° and 68.32 are due to diffraction from (1 0 0), (0 1 1), (2 0 0), (1 1 $\bar{2}$), (0 0 3), (2 1 $\bar{1}$), (2 0 3) and (0 3 1) planes respectively. All these peaks are due to feldspar minerals. Overall, majorly samples were having feldspar mineral and calcite. Silicate were the secondary component. Potassium aluminosilicate was also the major component of feldspar.

Based on thin section of the rock samples and powder X- ray diffraction analysis, a qualitative assessment of the mineral composition of the different monuments of the Champaner Pavagadh complex was done and has been indicated in table 5.9 below.

Table 5.9 – Qualitative assessment of the minerals on the different monument sites of Champaner Pavagadh complex

Sr. No.	Minerals	Makai Kothar	Jain temple	Antiquity	Navlakha Kothar
1.	Aluminosilicate	++	++	++	++
2.	Calcite	++	++	+	++
3	Orthoclase	+	-	+	+
4.	Plagioclase	+++	+++	+++	+++
5.	Muscovite	++	++	++	++
6.	Hematite and Magnetite	+++	++	+	++
7.	Silicates (Quartz)	+++	+++	+++	+++

High= +++ Medium= ++ Low= + (Qualitative concentration range)

The qualitative analysis revealed that the minerals plagioclase feldspar and silicates were dominant on the monuments located on the hill of the Pavagadh. This was followed by Hematite and Magnetite for the Makai Kothar and to a smaller extend for the Navalakha Kothar and the Jain temple. Orthoclase feldspar was very low as compare to other minerals while aluminosilicate and muscovite were more or less similar from the selected monuments.

5.1.4.3 Biofoulants with specific substratum

The amalgamation of the information of substrate composition and the distribution of different biofoulants on the different monuments was carried out to understand substrate specificity of the biofoulants. In current study, it was noticed that monuments of Champaner Pavagadh complex were made up from mainly mortar materials and each structure had a different composition.

Based on the tables 5.5, 5.6 and 5.8 we can realize that the cyanobacteria, *Leptolyngbya foveolarum* and *Nostoc punctiforme* and the bryophytes, *Hyophila involuta*, *Plagiochasma appendiculatum* and *Astellia angusta* were observed on both the Makai Kothar and the Navlakha Kothar which comprised of similar minerals with almost similar concentration. Similarly, the lichens, *Pertusaria multipuncta* and *Phaeophyscia hispidula* were found on both the Navlakha Kothar and the antiquity of the Jain temple and again both had a similar mineral composition. The substratum of buildings of MSU campus and the monuments at base of the Pavagadh hill were mainly made up of bricks, lime and mortar materials. Their geological study couldn't be carried out because a sample could not be obtained from the either the protected or the functional intact monuments. The table 5.10 below, depicts the substrate specificity for the different biofoulants encountered during the study.

Biodeterioration of Selected Historical Monuments by Lower Plants and Cyanobacteria

Table 5.10 – Biofoulants observed on specific substratum

Groups of Biofoulants	Substratum Type						
	Stone made up by different mortar materials				Mortar (Arts dome and Saher ki Masjid, Mandavi)	Lime (D.N. Hall and Mandavi)	Brick (D. N. Hall and Amir Manzil)
	Mortar 1 (Navlakha Kothar)	Mortar 2 (Makai Kothar)	Mortar 3 (Jain Temple)	Mortar 4 (Antiquity)			
Cyanobacteria	<i>Leptolyngbya foveolarum</i> , <i>Nostoc punctiforme</i>	<i>Leptolyngbya foveolarum</i> , <i>Nostoc punctiforme</i>			<i>Chroococcidiopsis cubana</i> , <i>Leptolyngbya foveolarum</i> , <i>Desmonostoc muscorum</i> ,	<i>Chroococcus varius</i> , <i>Chroococcus prescottii</i> , <i>Gloeocapsa palea</i> , <i>Gloeocapsopsis crepidinum</i> , <i>Aphanothece stagnina</i>	<i>Leptolyngbya crispate</i> , <i>Desmonostoc muscorum</i> ,
Microalgae			<i>Asterarcys quadricellulare</i>				
Bryophytes	<i>Anomobryum auratum</i> , <i>Fissidens splachnobryoides</i> , <i>Hyophila involuta</i> , <i>Semibarbula orientalis</i> , <i>Gymnostomiella vernicosa</i> , <i>Asterella angusta</i> , <i>Cyathodium cavernarum</i> , <i>Lejeunea aloba</i> , <i>Plagiochasma microcephalum</i> , <i>Plagiochasma appendiculatum</i>	<i>Hyophila involuta</i> , <i>Asterella angusta</i> , <i>Plagiochasma appendiculatum</i>		<i>Riccia gangetica</i> , <i>Riccia billardieri</i> , <i>Anthoceros bhadarwajii</i> , <i>Anthoceros subtilis</i> ,	<i>Hydrogonium arcuatum</i> , <i>Hyophila involuta</i>	<i>Hyophila involuta</i> , <i>Riccia discolor</i> , <i>Riccia billardieri</i>	<i>Fissidens splachnobryoides</i> , <i>Hyophila involuta</i> , <i>Riccia grollei</i> , <i>Gymnostomiella vernicosa</i>
Lichens	<i>Caloplaca awasthii</i> , <i>Pertusaria multipuncta</i> , <i>Diploschistes</i> , <i>Lepraria lobificans</i> , <i>Endocarpon nanum</i>	<i>Caloplaca cupulifera</i>	<i>Pertusaria multipuncta</i> , <i>Phaeophyscia hispidula</i>	<i>Lepraria coriensis</i>			

Biodeterioration of Selected Historical Monuments by Lower Plants and Cyanobacteria

Some species were recorded on more than one substratum while some were found on single substratum only. The analysis of the table 5.10 revealed that there was no specific correlation of species with substratum.

5.1.4.4 Status of Biofoulants on different substrates

At the beginning of the current study, it was assumed that there would be a high substrate specificity by the different species of cyanobacteria. However, this assumption has been proved wrong by the distribution results obtained in the current study. In current study, minerals like plagioclase, K-feldspar, calcite, quartz, mica and iron oxide minerals (magnetite and hematite) were obtained by XRD analysis of rock samples of some selected sites. Past study on XRD analysis of rock samples of Taj Mahal covered with black crust also revealed presence of same minerals named calcite, magnetite, hematite, mixed layer of silicates, plagioclase and microcline feldspar (Banerjee and Sarkar, 2019).

5.1.4.4.1 Cyanobacteria and green microalgae

The current study revealed that except *Chroococcidiopsis cubana* most of the cyanobacteria were found only on one substratum. Except *Aphanothece stagnina* all other members of Chroococcales were found to be growing on lime substratum. *Nostoc muscorum* and *Leptolyngbya foveolarum* were found to be growing on mortar while *Chroococcidiopsis cubana* were found to be growing on lime as well as on mortar substratum. Studies on various monuments in different parts of India have revealed that *Gloeocapsopsis cripendium* was recorded on lime stone (Samad and Adhikary, 2008 and Adhikary *et al.*, 2015), *Nostoc muscorum* on sandstone (Adhikary *et al.*, 2015), *Chroococcus prescottii* and *Chroococcus varius* on lime surface (Samad and Adhikary, 2008) and *Chroococcidiopsis cubana* from stone (Sahu *et al.*, 2011). In France, *Gloeocapsa palea* and *Leptolyngbya foveolarum* were recorded from building facades (Barberousse H. *et al.*, 2006). Similarly, Chen *et al.*, (2009) had reported the soil crust of cyanobacteria, mosses and lichens and also mineralogy wherein they observed minerals such as calcite, quartz, magnetite, plagioclase, microcline and mica.

5.1.4.4.2 Bryophytes

In current study, that maximum number of species of mosses and liverworts were recorded from the mortar surfaces. Earlier studies have reported the species of the order Pottiales followed by Bryales are known to take over the biofilm crust mosaics on mortar surfaces in Spain (Gil and Saiz Jimenez, 1992). Likewise, Jackson, (2015) analysed XRD of rock samples inhabited by bryophytes and lichens and found that rocks were having presence

Biodeterioration of Selected Historical Monuments by Lower Plants and Cyanobacteria

of potassium feldspar, plagioclase, quartz, calcite and mica (specially muscovite from mica category).

5.1.4.4.3 Lichens

These lichens were found from the different monuments but their minerals (calcite, quartz, feldspar, mica etc.) were almost same (Salvadori and Municchia, 2016). Plagioclase feldspar is dominant on monuments, where lichens were found (Seaward, 2001; Bajpai and Upreti, 2014). Latter it often replaced by ferruginous clay minerals. The lichens secretes oxalic acid and etches plagioclase feldspar and clay minerals to produced ochreus crust of ferruginous and alumina-silicate materials (Bajpai and Upreti, 2014). Similarly, current results also showed present of feldspar, ferruginous materials and alumina-silicate minerals, which might be scratches due to chemicals (acids or secondary metabolites) secreted by lichens causing the deterioration of the structures where were these minerals present. Because these chemicals having chelating properties, they are able to convert many minerals into water soluble complexes (Seaward and Richardson, 1989; Pinna, 1993).

5.2 Role of specific cyanobacteria, lichen and bryophytes in biodeterioration

5.2.1 Cyanobacteria

Cyanobacteria have the ability to survive in harsh environmental condition and can stay hydrated internally. A major reason for this is the capacity of these pioneering organisms to secrete polysaccharides into the external environment which are known as exopolysaccharides (Sureshkumar *et al.*, 2007; Nwodo *et al.*, 2012; Rossi and Philippis, 2015). Being mucilaginous in nature, the surface of the exopolysaccharide facilitates the attachment of propagules of others organisms which leads to further colonization of the surface by different organisms. In consequence, exopolysaccharide is the key player for the deterioration process. These exopolysaccharides are composed of several different sugars in different combinations (Sutherland, 1999; Nishanth *et al.*, 2020). Hence, this present study focussed on characterization of the principal sugars in their extracellular polysaccharides matrix and their role in deterioration.

5.2.1.1 Extraction of EPS, its Confirmatory test and Acid hydrolysis

Exopolysaccharides are secreted on the outer side of the cells as slime or released polysaccharides (RPS). Extracted exopolysaccharide pellets were visualized as white in colour shown in fig.5.12 (A). Impurity of other extracellular material like DNA, protein etc. is a possibility for these pellets and hence, the purity of the EPS pellets was confirmed using

Biodeterioration of Selected Historical Monuments by Lower Plants and Cyanobacteria

the confirmatory test of total carbohydrate (Fig. 5.12 – B and C). Preliminary extracted exopolysaccharide did not show the presence of any carbohydrate because test solution did not change the colour and remained the same as control (Fig. 5.12 – Tubes D1 & D2). After repeatedly trying for extraction of exopolysaccharide, pure carbohydrate pellet of exopolysaccharide was obtained. This was confirmed from the different shades of bluish colour of the solution as per standard solution shown in fig. 5.12 representing tubes D3, D4, D5 and D6. Tube D4 had got exact colour same as monosaccharides standard glucose. Whereas, tubes D3, D5 and D6 had little different shades of bluish yellowish. This test confirmed the purity of the sample. These pure exopolysaccharide samples were acid hydrolysed for further analysis. The hydrolysed exopolysaccharide samples were used for HPTLC analysis.

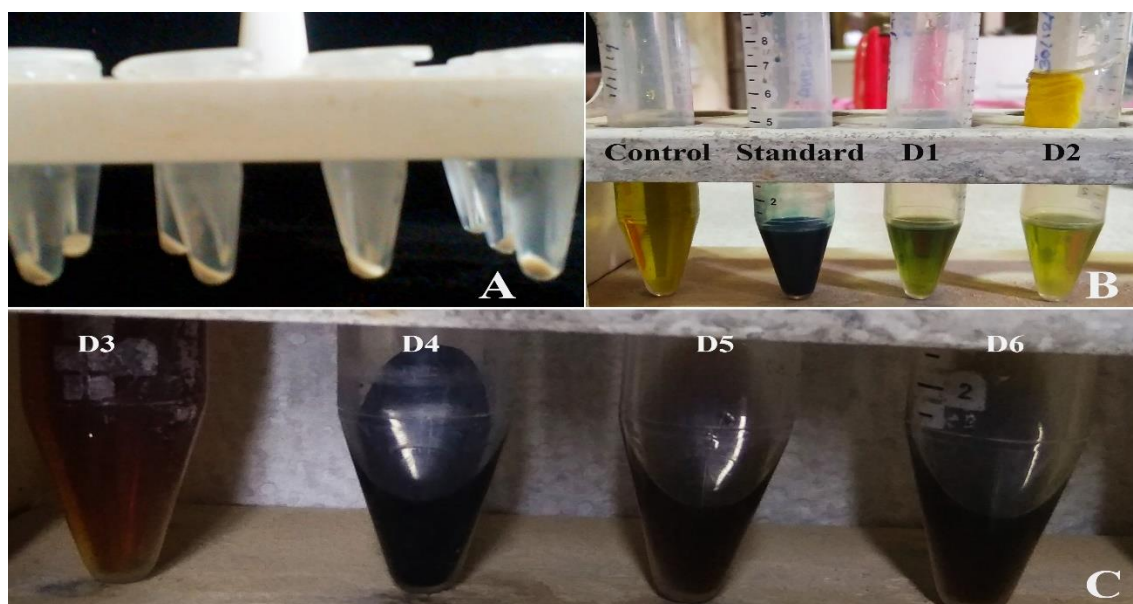


Fig. 5.12 – A. EPS pellets B. & C. Confirmatory test of total carbohydrate

5.2.1.2 Determination of monosaccharides by HPTLC analysis

The HPTLC method provided a fingerprint profile chromatogram by densitometric evaluation. Using this method, the EPS of the six main isolated biofoulants were analysed which revealed the presence of heteropolysaccharides. The method allowed the generation of three sets of R_f values for each compound which facilitated the separation of compounds which has similar max R_f values. Comparison with standards R_f values (Table 5.9) and colour of the fingerprints after derivatization indicated the presence of specific monosaccharides in the EPS which were confirmed based on their various R_f values and peaks of spectra obtained at 366 nm. The obtained spectra of all tracks are shown in fig. 5.14.

Biodeterioration of Selected Historical Monuments by Lower Plants and Cyanobacteria

The obtained chromatograms were viewed at two different wavelengths of 580 nm and 366 nm which have been depicted at fig. 5.13 A and B respectively.

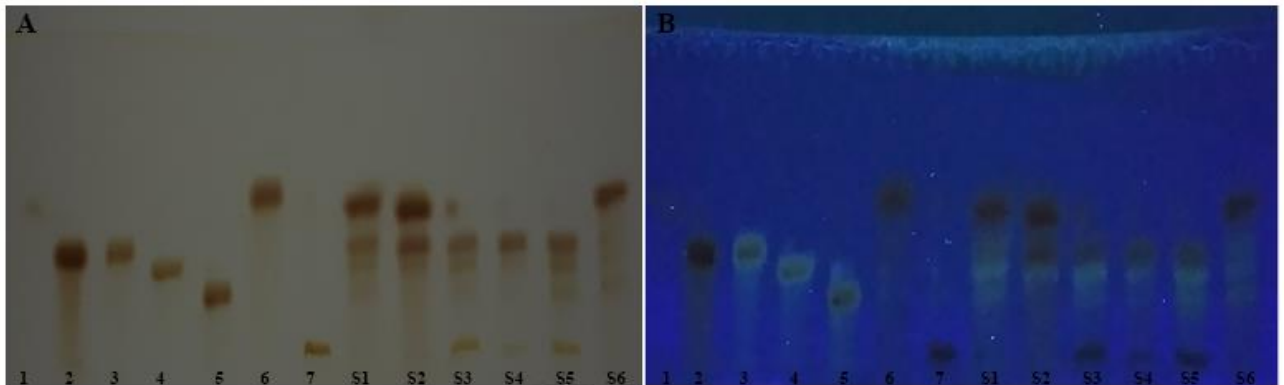


Fig. 5.13 – HPTLC fingerprints of exopolysaccharides of Champaner Pavagadh complex biofoulants

1-Xylose, 2-Arabinose, 3-Mannose, 4-Glucose, 5-Galactose, 6-Fucose, 7-Galacturonic acid, S1- *Desmonostoc muscorum*, S2- *Nostoc punctiforme*, S3- *Leptolyngbya crispata*, S4- *Leptolyngbya foveolarum*, S5- *Chroococcidiopsis cubana*, S6- *Asterarcys quadricellulare*

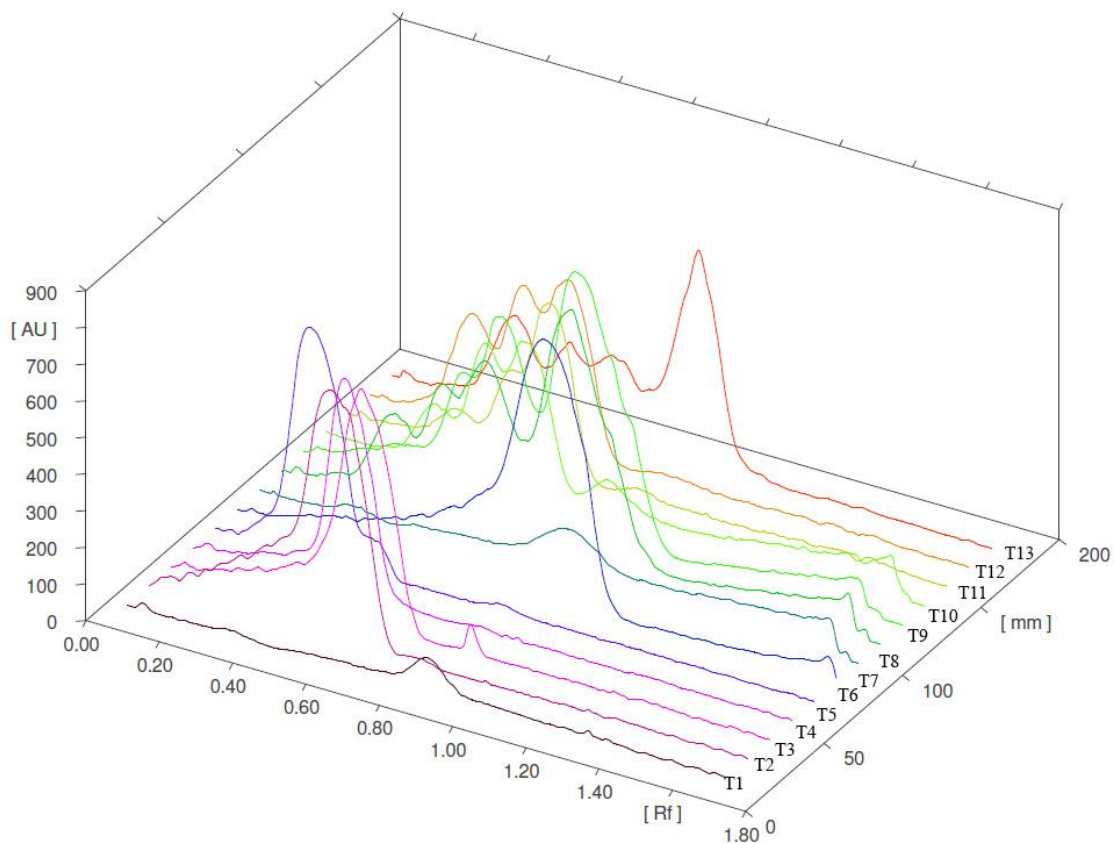


Fig. 5.14 – Spectra of all tracks at 366 nm

Biodeterioration of Selected Historical Monuments by Lower Plants and Cyanobacteria

The analysis revealed the presence of six neutral sugars (fucose, xylose, mannose, glucose, arabinose, galactose) and one sugar acid (uronic acid). Each strain had the presence of three to five monosaccharides. HPTLC fingerprint profile and peak of the spectra revealed that hydrolysed exopolysaccharides of *Desmonostoc muscorum* had mannose, fucose, glucose and galactose (visualized in 366 nm); *Nostoc punctiforme* had arabinose, glucose, fucose; *Leptolyngbya crispata* – xylose (not visualized in 366 nm), arabinose, glucose, galactose (visualized in 366 nm), galactouronic acid; *Leptolyngbya foveolarum* – Arabinose, glucose, galactose, galactouronic acid; *Chroococciopsis cubana* – arabinose, glucose, galactose, galactouronic acid and *Asterarcys quadricellulare* – fucose, mannose, glucose, galactose (Mehta *et al.*, 2021). Xylose wasn't observed in image taken by 366 nm. It was visualized in white light. Likewise, galactose wasn't clearly observed in white light but was clearly visualized in 366 nm.

Glucose and galactose (except in S2) were found in all biofoulants exopolysaccharides. Xylose was visible at 580 nm only and hence has not been included in table 3 which indicates the area covered values observed at 366 nm. Xylose was found in only one species, *Leptolyngbya crispata*. Fucose was found to be more predominant as the percentage area was 48.37%, 51.09% and 48.83 % as compare to other monosaccharides. After fucose, the covered percentage area (Table 5.12) indicated that arabinose and mannose were also present in significant concentrations. The area under the graph covered by galacturonic acid was small indicating it to be present in small amounts.

Table 5.11 – Rf values of monosaccharides peak at 366 nm wavelength

Monosaccharides	Start Rf	Max Rf	End Rf
Xylose	0.75	0.87	0.96
Arabinose	0.51	0.59	0.76
Mannose	0.53	0.60	0.73
Glucose	0.37	0.50	0.59
Galactose	0.21	0.36	0.46
Fucose	0.73	0.84	1.1
Galacturonic acid	0.78	0.86	1.07

Table 5.12 – Area covered by peaks at 366 nm of each monosaccharide in all samples

Sample tracks	Area covered (%)					
	Arabinose	Mannose	Glucose	Galactose	Fucose	Galacturonic acid
S1	-	23.27	12.79	10.73	48.37	-
S2	26.68	-	11.25	-	51.09	-
S3	35.85	-	27.14	11.86	-	8.31
S4	63.14	-	20.50	11.82	-	2.07
S5	42.70	-	29.50	26.30	-	0.63
S6	-	16.69	13.84	20.25	48.83	-

5.2.1.3 Status of Exopolysaccharides study

Monosaccharides from the EPS of different bacterial and microalgae strains have been separated using various methods such as ion exchange chromatography, GC/MS, HPLC with refractive index detection and LC-High resolution Mass Spectroscopy (LC-HRMS) (Khattar *et al.*, 2010; Rossi *et al.*, 2012; Delattre *et al.*, 2016; Baldev *et al.*, 2015). In these methods the separation of sugars (e.g. glucose and mannose) with a similar retention time was difficult and they had to be subsequently confirmed using TLC (Khattar *et al.*, 2010; Baldev *et al.*, 2015). HPTLC technique has been used as a very sensitive visual method for the rapid and precise differentiation of compounds (Makowicz *et al.*, 2018). In the present study, the HPTLC method has been used for the first time for separation of exopolysaccharides sugars from cyanobacteria and microalga. HPTLC method used in the current study proved to be more accurate and rapid as it provided results in the form of both spectra as well as chromatogram with different Rf values.

In current study, we had found total seven monosaccharides from all the strains of cyanobacteria and one microalga using HPTLC technique. The EPS of several microalgae and bacterial groups like Bacillariophyta, Charophyta, Chlorophyta, Haptophyta, Cyanobacteria, Miozoa and Rhodophyta have reported a presence of a minimum of two and up to a maximum of nine monosaccharides (De Philippis *et al.*, 1998; Hu *et al.*, 2003; Kielme *et al.*, 2007; Pereira *et al.*, 2009; Pignolet *et al.*, 2013; Raposo *et al.*, 2015;). The EPS of most cyanobacteria are moderately complex as compare to other bacteria and microalgae, and are

Biodeterioration of Selected Historical Monuments by Lower Plants and Cyanobacteria

generally composed of six or more monosaccharides (Chug and Mathur, 2013). While in some case, two to three monosaccharides were also reported from EPS of cyanobacteria (Parikh and Madamwar, 2006). Kielme *et al.*, (2007) reported eight neutral sugars and rarely one uronic acid from released polysaccharides of microalgae.

In the present study, we had observed three to five monosaccharides from each species. We had noted majorly arabinose, glucose, galactose and either fucose or galactouronic acids from EPS of presently studied strains. Gloaguen *et al.*, (1995), De Philippis *et al.*, (1998) and Parikh and Madamwar, (2006) had observed major neutral sugars like glucose, mannose, arabinose and xylose from cyanobacteria. Rossi F. *et al.*, (2012) had reported the presence of fucose, rhamnose, galactosamine, arabinose, glucosamine, galactose, glucose, xylose, fructose, ribose, galacturonic acid and glucuronic acid from the EPS of *Leptolyngbya*. Presently studied EPS of *Leptolyngbya* species had found arabinose, glucose, galactose, galactouronic acid and xylose. In current study, *Nostoc* species had found arabinose, mannose, glucose, galactose, fucose while Parikh and Madamwar, (2006) reported only two monosaccharides xylose and mannose from EPS of *Nostoc* species. EPS of green microalgae usually have arabinose, rhamnose, fucose, ribose, xylose and galactose (Kielme *et al.*, 2007; Delattre *et al.*, 2016). While in present study mannose, glucose, galactose and fucose were noted from released polysaccharides of *Asterarcys quadricellulare*, a green microalga. Glucose was identified in the EPS of all the biofoulants but it was not observed as major component. Rossi *et al.*, (2012) and Khattar *et al.*, (2010) had also found the presence of glucose in all the strains studied. EPS quantification of biocrust samples were recorded by Mugnai *et al.*, (2020). They had reported glucose (54% molar) as dominant component of EPS of biocrust samples. The current study results reveal that fucose (51% area covered) and arabinose (63% area covered) were the dominant monosaccharide wherever they were present (Table 3). Galacturonic acid was present in 50% samples of the present study and had a minimal amount (0.63 to 8 % area covered) as compare to other monosaccharides. Similar results were obtained by Mugnai *et al.*, (2020). They had also not detected galacturonic acid in one sample out of six biocrust samples. Moreover, they were also recorded that galacturonic acid was present in minimum quantity (0.87 to 34 % molar). In current study, we also studied some relationship of monosaccharides. For example, arabinose and mannose as well as fucose and galacturonic acid were disjoint i.e., they both could not observed at the same species (simultaneously). Glucose was however found in greater proportion than galactose in all members isolated except *Asterarcys quadricellulare* which is a microalga.

But this kind of relationship between monosaccharides has not been reported in earlier studies.

5.2.2 Bryophytes

In bryophytes, the presence of fixed negative charges on the cell wall imparts it an important role in the uptake of some nutrients and non-essential cations (Wells and Brown, 1987; Bates, 1992). The percentage of polysaccharides in cell wall does not vary among the bryophytes (Inoue *et al.*, 1981; Bates, 1992) but the difference in the degree of esterification of carboxyl group varied in cation exchange capacity (CEC) between the bryophytes (Rouzere *et al.*, 1986; Bates 1992). Calcium is one of the exchangeable cation. This cation fixes with negative charges of carboxyl groups of pectin polysaccharides in the matrix of the cell wall. Normally Ca^{+2} can be displaced and assayed by supplying at high concentration of firmly bound cation Sr^{+2} or Ni^{+2} (Bates, 1982). The role of bryophytes in biodeterioration was studied using one liverwort (*Asterella angusta*) and one moss (*Hyophila involuta*) that were commonly available and dominant on monuments of the study sites.

5.2.2.1 Analysis of Calcium uptake from apoplast regions (intercellular level)

The apoplast is the region outside the plasma membrane and space in between the cells within which material can diffuse freely. Uptake chemicals are easily trapped in this region and can be utilized for the growth of plants. Analysis of the Calcium uptake by *Hyophila involuta* and *Asterella angusta* from geological substratum was done through flame photometry and their response values were calculated from calibrated (standard) graph showed in fig. 5. When the solution tube was kept at 20 °C no response was obtained but a clear response was obtained on the digital screen when the solution tube was kept at 37 °C. The concentration of the calcium was calculated based on the responses obtained for each samples using the equation obtained from the standard calibration graph given in fig. 5.15 below.

Calculation

$$y = 0.8157x - 0.4506 \quad \dots \text{equation 5.2}$$

Where, x = Calcium concentration (ppm) and y = Response on flame photometer

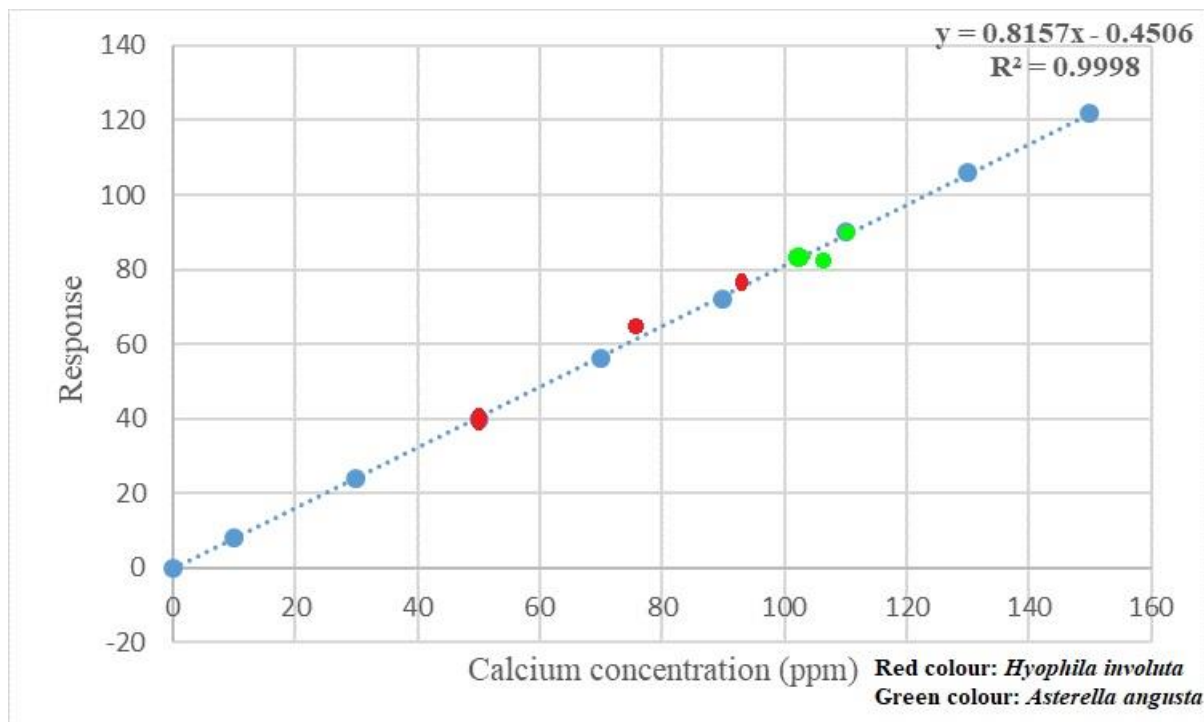


Fig. 5.15 – Values of Calcium concentration (ppm) obtained in *Hyophila involuta* and *Asterella angusta* overlaid over the standard calibration curve.

Based on calculation, the average value of calcium uptake by *Hyophila involuta* (moss) was 72.88 ppm and by *Asterella angusta* (liverwort) was 105.54 ppm. Taking into consideration the amount of plant material taken for the experiment the Calcium uptake was 0.052 mg per mg for plant samples of *Asterella angusta* while it was 0.036 mg per mg for plant samples of *Hyophila involuta*.

5.2.2.2 Status of calcium Uptake study in bryophytes

The mechanical and chemical deteriorative action shown by these organisms on monuments is negligible, as they do not have true roots systems but having rhizoids which are not directly in contact with stone surface, even if the capacity of mosses to accumulate Ca^{+2} ions could be related with a biodeterioration capacity (Keller and Frederickson, 1952; Tiano, 2002). There were very few studies regarding calcium ion exchangeable by mosses. In current study, the calcium cation exchange analysis was done in *Hyophila involuta* (moss) and *Asterella angusta* (liverwort). This calcium cation exchange analysis is a first time approach for liverworts. Earlier this analysis was done in moss *Pleurozium schreberi* growing in Windsar forest, U.K. and *Grimmia pulvinata* growing on structures made up of marble and travertine (Bates, 1992; Altieri and Ricci, 1997). In current study, calcium uptake perceived 52 $\mu\text{g}/\text{mg}$ plant samples of *Asterella angusta* and 36 $\mu\text{g}/\text{mg}$ plant samples of *Hyophila*

Biodeterioration of Selected Historical Monuments by Lower Plants and Cyanobacteria

involuta. Bates, (1992) reported Ca⁺² exchangeable cation 55 µmol/g and Altieri and Ricci, (1997) mentioned calcium uptake 6 mg/g plant and 3 mg/ g plant of the species *Grimmia pulvinata* growing on marble and travertine respectively. In present study, it was noticed that more calcium was absorbed by liverwort *Asterella angusta* as compare to moss *Hyophila involuta*.

5.2.3 Lichen

Lichens contributed to the deterioration process by physical and chemical processes. Studies on biodeterioration highlighted the possible effect of dissolved carbon dioxide derived from lichen respiration, attacking the substratum to produce pits and channels for easier penetration of hyphae. Based on a chemical perspective, lichen acids have relatively low solubility, but they are effective chelators forming metal complexes with silicates and other minerals derived from the substratum (Seaward, 2001). Other than atmospheric carbon dioxide, some other acids secreted by lichens are also responsible for the deterioration process by lichens.

5.2.3.1 Secondary metabolites based on chemical spot test and literature

Lichen acids are mainly polyphenolic compounds in two different forms, aliphatic and aromatic. Aliphatic polyphenolic compounds contain fatty acids, polyols and triterpenoids while aromatic are having tetronic acid derivatives, depsides, depsidones, quinons, dibenzofurans and diketopiperazine derivatives (Bajpai and Upreti, 2014). To know the presence of these acids, chemical spot tests and TLC of samples in different solvent are generally needed. Chemical spot tests are used to detect the presence of certain unspecified lichen chemical substances by colour reactions of lichen tissues. They are also used for determining the localization of chemical substance. It is very rapid and convenient method to perform even in field conditions, especially where the material can't be collected conveniently (Orange *et al.*, 2001). In the current study, sufficient samples of lichens to carry out Thin layer chromatography (TLC) could not be collected (as they were growing on protected monuments). Hence, in current study, the chemical spot tests were performed at field locations and the results have been depicted in the images shown in plates 22 (Fig. D) and 23 (Fig. C). The resulting colour observed and noted wherever it was detected. The colour detected in *Caloplaca awasthii* and *Caloplaca cupulifera* was K⁺ purple and K⁺ red respectively. A K test red generally indicates that the O – hydroxyl aromatic aldehydes could be present. While K test bright red to purple suggested the reaction with anthraquinone pigments (Bajpai and Upreti, 2014). The remaining observed lichens from the monuments did

Biodeterioration of Selected Historical Monuments by Lower Plants and Cyanobacteria

not show any colour in chemical spot test. Thus the results for *Lepraria coriensis*, *Lepraria lobificans*, *Diploschistes* sp., *Endocarpon nanum*, *Pertusaria multipuncta* and *Phaeophyscia hispidula* were noted as K-, C-, KC-, and PD-. Several references were reviewed for the presence of other chemicals in the species present. The available literature indicated the possible presence of three aromatic polyphenolic compounds such as Parietin (*Caloplaca awasthii*, *C. cupulifera*), Atranorin and stictic acid (*Lepraria lobificans*) and one aliphatic polyphenolic compound like zeorin (*Lepraria lobificans* and *Phaeophyscia hispidula*) from the specimens collected from the study area (Bajpai and Upreti, 2014; Shukla *et al.*, 2014). These secondary metabolites viz. Parietin, Atranorin, Stictic acid and Zeorin belong to different groups like quinones, depsides, depsidones and triterpenes respectively. Zeorin has the potential to cause damage to the substratum by chelation action (Clair and Seaward, 2004) while Atranorin and Parietin can potentially leach to the substratum causing damage the substratum of the monument (Chen *et al.*, 2000).

Based on this survey, it is possible that these aromatic polyphenolic compounds were playing a major role in the deterioration of Champaner Pavagadh monuments. These water soluble phenolic compounds play important role in metal chelation (Culberson, 1969; Shukla *et al.*, 2014). Sometimes, oxalic acid reacts with calcium in lichens, particularly those species inhabiting on calcareous materials. Because of this reaction, excreted oxalic acid by lichens form calcium oxalate (Chen *et al.*, 2000). This calcium oxalate layer has been frequently observed on the monuments made up of calcareous materials. As a result, these compounds oxidized the organic materials, which can originate through very slow but spontaneous chemical reactions such as mineralization process (Matteini and Moles, 1986).

5.1.3 Measures for controlling the biodeteriogens

The protection of monuments from the activities of microorganisms was the emphasis of the current study. A group of *in-vivo* experiments to test the efficacy of different control measures was devised from the available literature. However due to the COVID-19 pandemic the experiment could start in October 2020. Two different chemicals were selected based on their physical properties like colour, transparency and water repellent capacity after literature survey (Tsakalof *et al.*, 2007; Sadat-Shojai and Ershad-Langrouddii, 2009; Gupta and Sharma, 2011; Tewari, 2016; Soulios *et al.*, 2019) and interaction with conservation experts from the ASI's Aurangabad circle (Dr. Deepak) and Hyderabad circle (Dr. Tahir). Two chemicals that possessed the above properties were selected. They are silane-siloxane based compounds and their trade names are BS 290 and SMK 1311(Wacker). The experiment was undertaken on

Biodeterioration of Selected Historical Monuments by Lower Plants and Cyanobacteria

the dome of the Arts Faculty building of the MSU campus. As described in the methodology, sites were selected in the four cardinal directions and the experiment was conducted. Visual observations were collected from each site every month. Photographs showing the status of the experimental sites were taken for each treatment in each direction and have been represented in the plates 30, 31, 32 and 33 respectively.

Each plate indicates the status of biofouling at the start of the experiment and observation made with the passage of time. Every month at the fixed date the sites were visited and checked for the growth of biofoulants. The observations ran from October to May which coincided with the non-favourable period and June to August which correspond favourable period for the growth of cyanobacteria. During favourable period of cyanobacterial growth small changes were observed in some treatments. The status of the changes has been depicted in the respective plates. The status of the substratum at the beginning of the experiment has been depicted in the top row of each plate which has been marked as untreated. The second row which is just below the label ‘outcome of experimental work’ and has the label ‘Initial phase’ shows the status of the experimental site just after the treatment has been completed. The rows below it depict the visual observations that were made for the months November (2020) and January, March, May, July August (for the year 2021) for each experimental site. The treatments that each site were subjected to have been indicated in the table 5.13 below.

Table 5.13 – Demonstrated different treatments for *in vivo* experiment on the Dome surface

Sr. No.	Different Treatments	Name of the Treatments
1.	A	Rubbing
2.	B	Rubbing + Spraying Ammonia solution
3.	C	Rubbing + Spraying Ammonia solution + Sodium penta chloro phentate
4.	D	Rubbing + Spraying Ammonia solution + Sodium penta chloro phentate + Wacker BS 290
5.	E	Rubbing + Spraying Ammonia solution + Sodium penta chloro phentate + Wacker SMK 1311

5.1.3.1 Outcome based on the directions

Each direction has different sun light orientation. For example, the east and west directions have sun light falling directly while for the north and south directions the light comes at a specific angle and in different season sunlight does not reach due to changes in the sun angle. Hence it was expected that the results would vary in each direction because some organisms grow and survive in direct sun light or some organisms prefer shades for their optimal growth. Direct sunlight or shades are either favourable or non-favourable depend on the organisms. Because in these situations organisms grow and survive in such harsh conditions also due to their outer complex layer. Based on the directions point of view, the west direction showed positive results in all over treatments followed by South, East and North directions.

5.1.3.2 Outcome based on the treatments

All these different treatments have different outcomes. These different outcomes were compared based on the different criteria such as reappearance of biofilm growth, any additional biofilm patches observed as compare to the initial phase of treatments, size of the biofilm patches etc. Based on all these criteria, from all over the treatments, treatment E has given best results throughout the observation periods in each directions. Treatment C followed by D treatment had also given satisfactory results in each directions across the observation periods. On the site of treatment A, the biofilm growth reappeared in all the directions in the month of July and August. But more patches of biofilm were observed in the north and east directions followed by west and south. The enlarged view of the regrowth of the biofilm in the month of July and August from the north and east directions (Fig. 5.16).

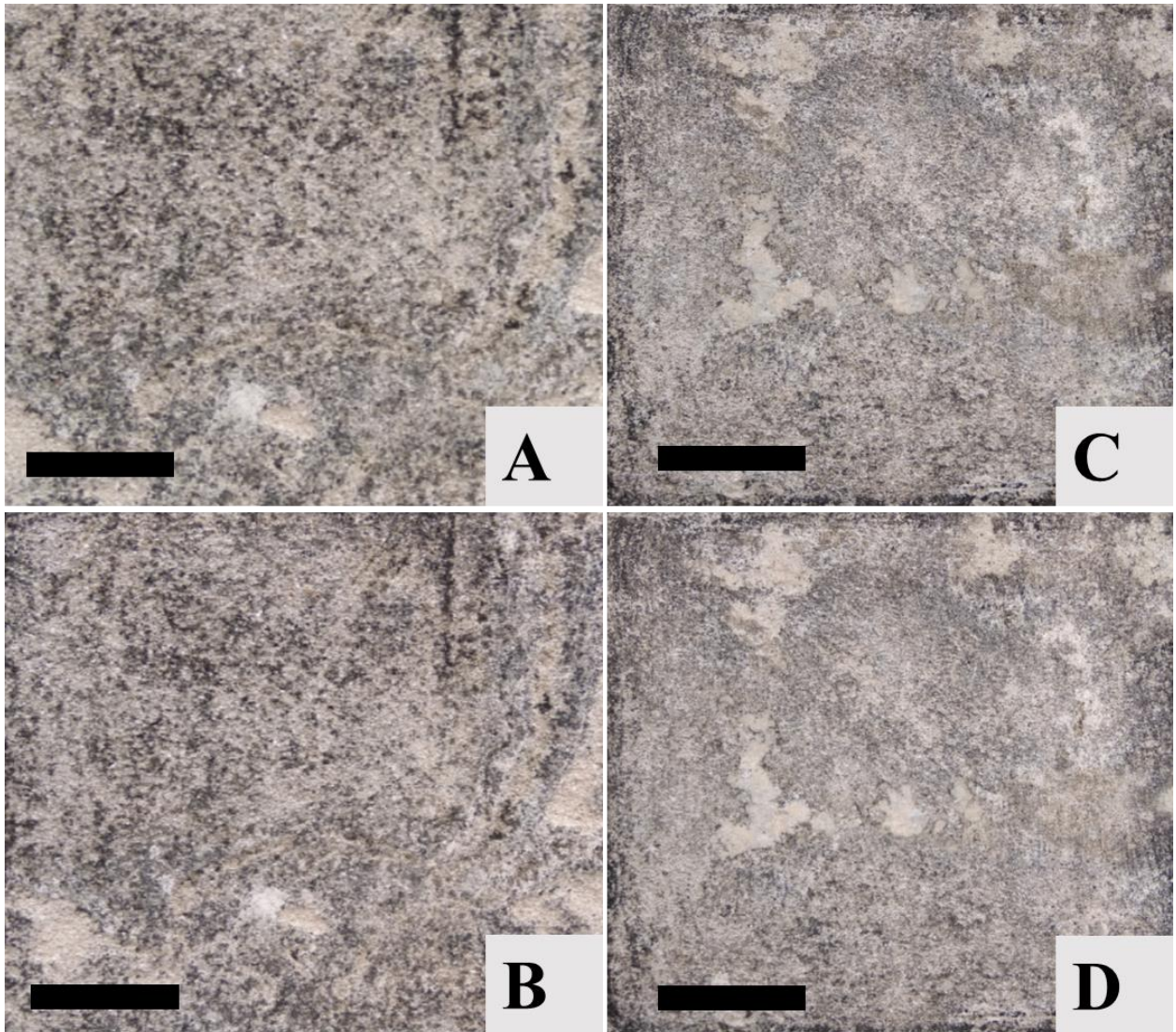


Fig. 5.16 – Enlarge view showing the biofilm regrowth on the place of treatment A. A, North direction July observation; B, North direction August observation; C, East direction July observation D. East direction August observation (Scale bar for all images = 3 mm)

5.2.4 Status of Control Measures study

Nowadays, conservation of the monuments is globally challenging. Because many reasons are causing the deterioration on the monuments. The current study is focused on the deterioration by biological organisms invading on the monuments and degrading the structures. Moreover, many government and non-government organizations are working on it. But from those organizations, several are not restored by scientific approach and very few are doing by chemical conservation. Thus, in current study, water repellent compound was

Biodeterioration of Selected Historical Monuments by Lower Plants and Cyanobacteria

used for conservation. Because the growth of biological organisms cannot occur on the surface having water repellent property.

In current study, *in vivo* experiment on the dome of the Arts building had obtained significant result in the treatment E (coating of Wacker SMK 1311) throughout observation periods because of the water repellent property of the selected chemical. Followed by treatment C (Sodium penta chloro phentate) and treatment D (Wacker BS 290). Because all these treatments had not showed the regrowth of the biofilm as compared to the initial phase of the experiment. These treatments were done on the dome surface which was made up of sandy limestone material. Internationally, similar kind of material (sandy limestone) at Madara plateau in Bulgaria was conserved through the Wacker silicones 290 by the researchers Hristova and Todorov (1996). Tsakalof *et al.*, (2007) investigated the efficiency of different types of siloxane and siloxane/acrylate based polymer coatings which were commercially available and used for the preservation of stone substrates of the monuments. Chang *et al.*, (2001) investigated BS 290 and SMK 1311 as water repellent on the swelling minerals such as smectite. Chang *et al.*, (2004) studied the BS 290 water repellent for the preservation of smectite rich rocks. Soulios *et al.*, (2019) used the BS 290 and SMK 1311 for the study of hydrophobic impregnation on the collected exposed building materials.

In India, Gupta and Sharma (2011), Tewari (2016), Kumar *et al.*, (2016) and the team of ASI members selected Wacker BS 290 widely for the preservation of some selected monuments of Tamilnadu, Chhattisgarh, Nashik and very few monuments of Gujarat. They had mentioned that BS 290 was water repellent and stopped water settling on the stone surface.

In current study, the selected chemicals for the different treatments were also water repellent. With the amount of observations that have been possible we can infer that SMK 1311, Sodium penta chloro phentate and BS 290 had given substantially good results.

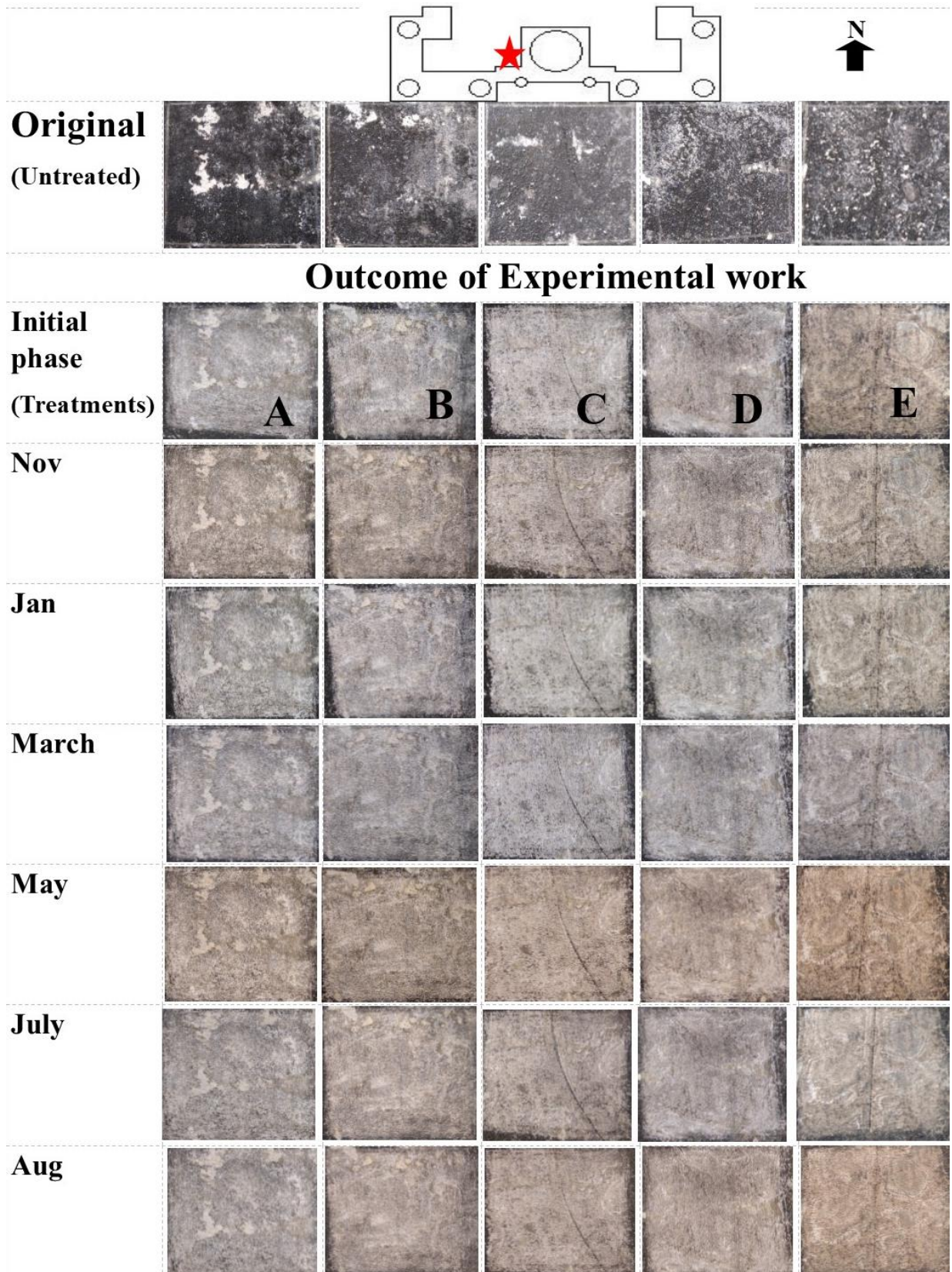


Plate 30 – Outcome of East direction of *in vivo* experiment work on Dome surface of the Arts building

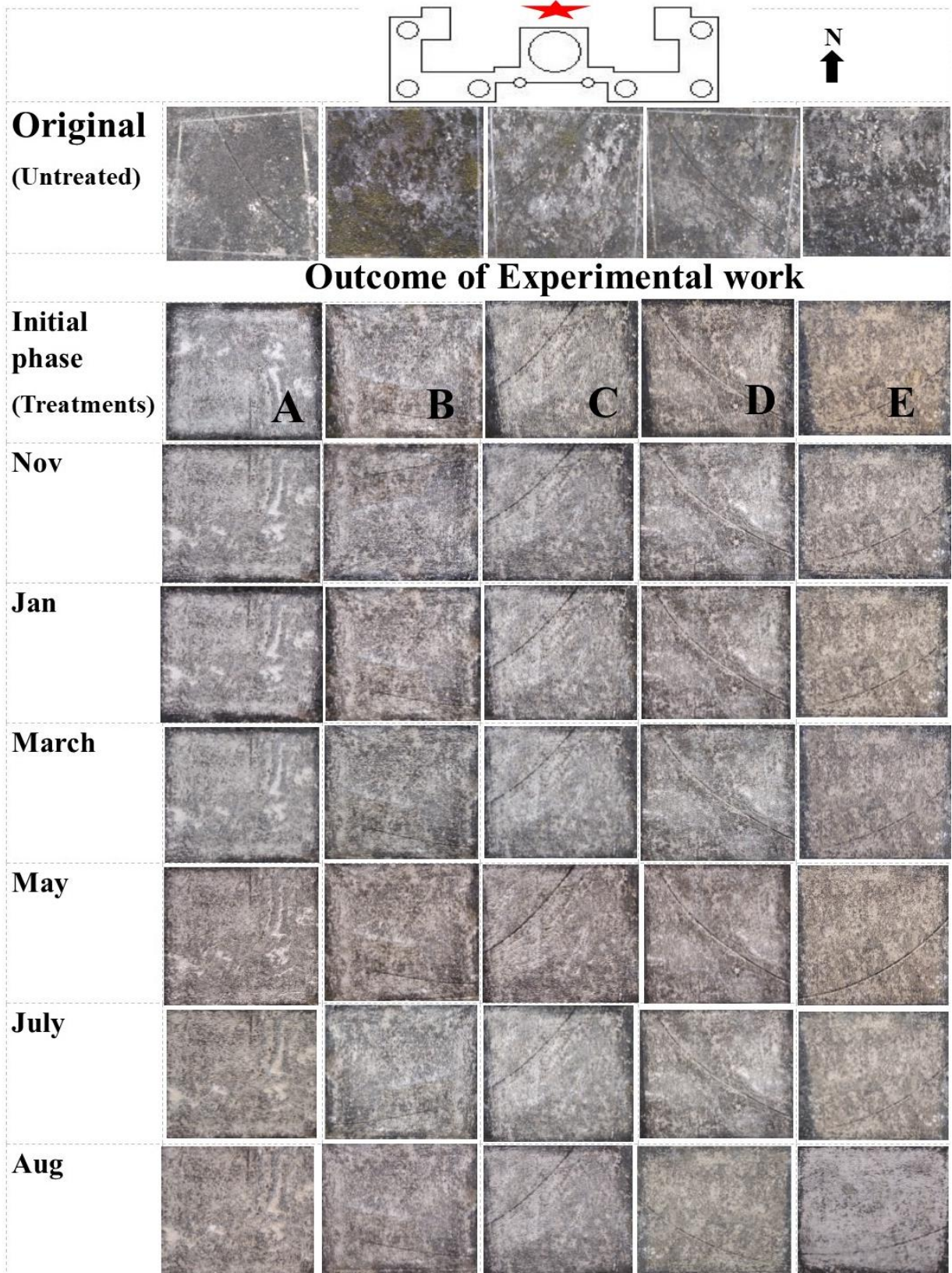


Plate 31 – Outcome of North direction of *in vivo* experiment work on Dome surface of the Arts building

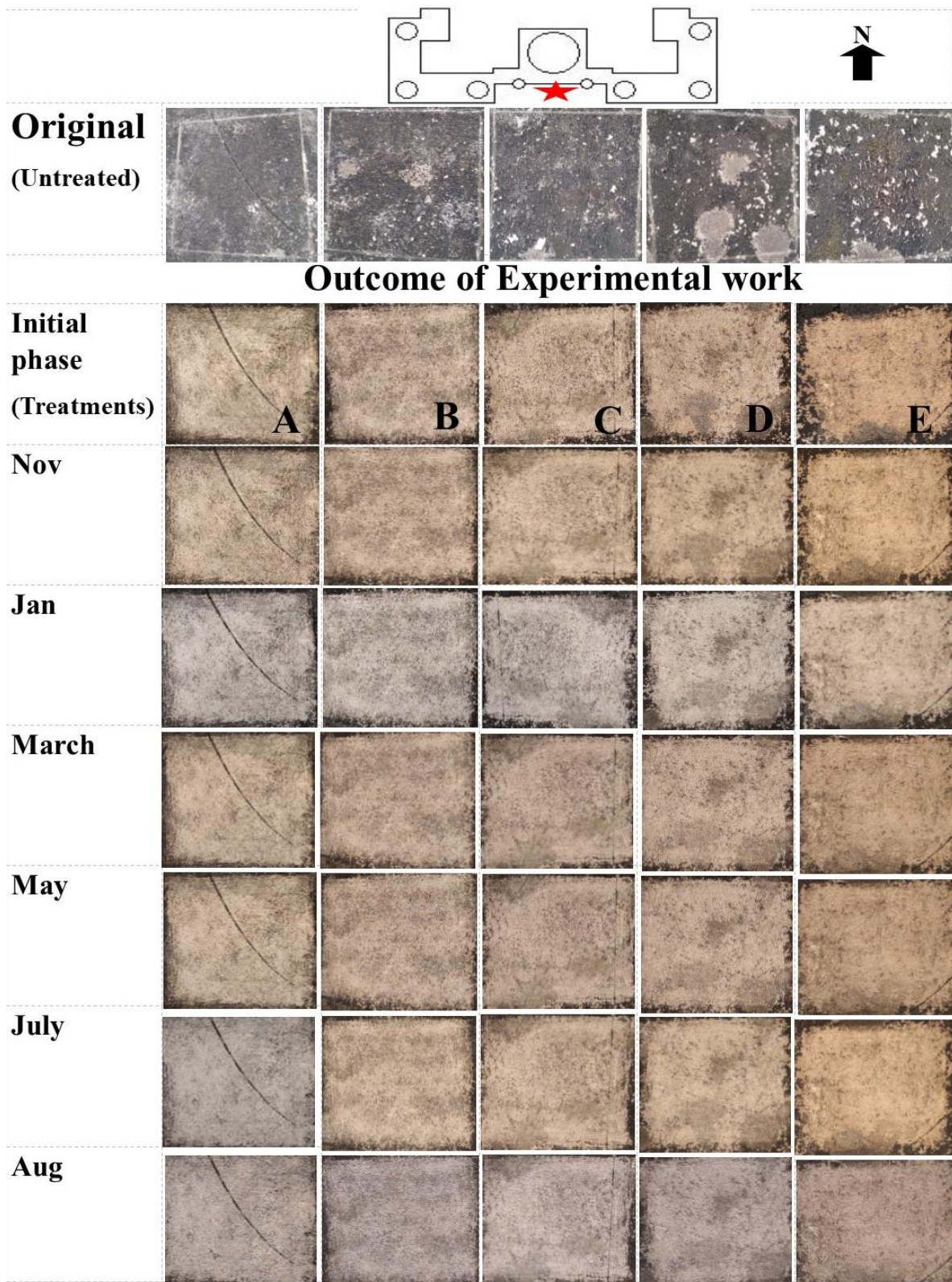


Plate 32 – Outcome of South direction of *in vivo* experiment work on Dome surface of the Arts building

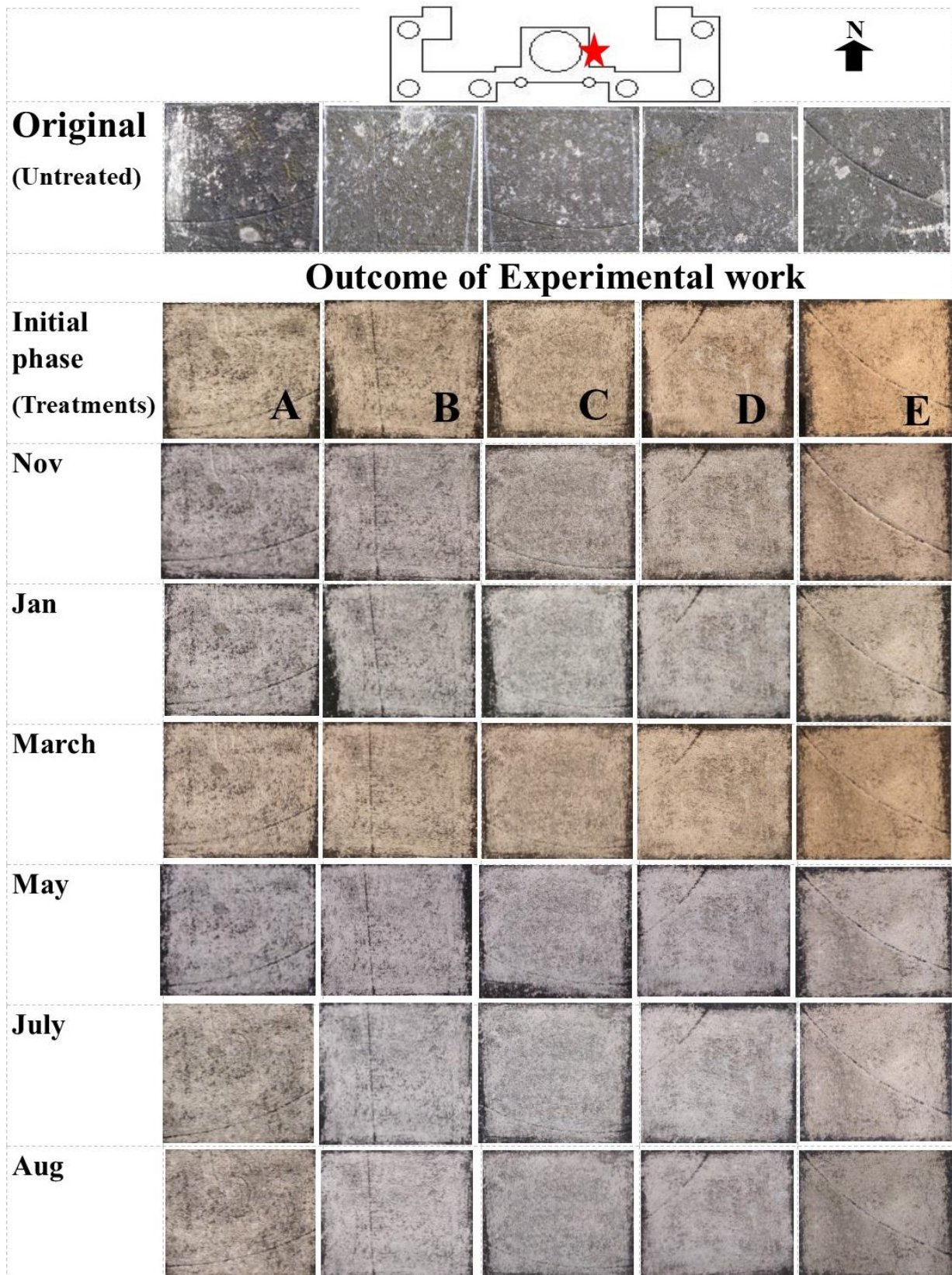


Plate 33 – Outcome of West direction of *in vivo* experiment work on Dome surface of the Arts building